



Wrocław University of Technology

TYPE III SOLAR CELLS BASED ON QUANTUM DOTS

To be presented as an aspiration for the degree of
Bachelor of Science

Maksymilian Kliczkowski

Faculty of Fundamental Problems of Technology
Wroclaw University of Science and Technology
Poland
December 27, 2019



Wrocław University of Technology

TYPE III SOLAR CELLS BASED ON QUANTUM DOTS

Supervisor
prof. dr hab. inż. Artur Podhorodecki

Faculty of Fundamental Problems of Technology, Experimental Physics Cathedral
Wroclaw University of Science and Technology
Poland
December 27, 2019

ABSTRACT

In this thesis the extensive review of possible and surely optimal materials for Quantum Dot Solar Cells (QDSCs) will be provided to the reader. One will have the opportunity to develop a rather current image of the necessary parts in their architecture which will be supported with an abundant description of the important aspects in engineering a photovoltaic device. With an introduction of its kind we will try to convey a basic but sufficient knowledge of standard terms, light with matter interaction, light spectrum analysis, quantum dots description with their behaviour and a photovoltaic device operation theory. It will be supported by certainly needed quantities that one has to find in order to properly describe a solar cell. With the objective of creating a possibly competitive Quantum Dot Sensitized Solar Cell(QDSSC) the description of methods that we used will be included with a related to it characteristics. One will also be able to use this paper as a review of today's development phase and current technological state of the other scientific groups all around the world. After a successful development of a solar cell, the analysis will definitely be provided.

STRESZCZENIE

W tej pracy zajmiemy się przeglądem optymalnych materiałów, na podstawie których możliwe jest tworzenie ogniw słonecznych bazujących na kropkach kwantowych. Dzięki temu pokazany zostanie obecny obraz zawierający opis wspomnianych wcześniej materiałów oraz przedstawiony zostanie wstęp dotyczący projektowania tychże urządzeń. Wraz ze wstępem zawarte zostaną wystarczające podstawy oddziaływanie światła z materią, analizy spektralnej, opisu kropek kwantowych, czy też działania urządzeń fotowoltaicznych. Podczas gdy głównym celem jest stworzenie jak najbardziej konkurencyjnego urządzenia, możliwe będzie również zapoznanie się z zastosowanymi metodami. Dodatkowo, w pracy zaprezentowano krótki przegląd obecnego rozwoju technologii związanych z QDSSC na całym świecie. Po wykonaniu urządzenia przeprowadzona zostanie także analiza otrzymanych wyników.

DEDICATION

To my , family and friends...

DECLARATION

I hereby declare that the present bachelor's thesis was composed by myself and that the work contained herein is my own. I also confirm that I have only used the specified resources. All formulations and concepts taken verbatim or in substance from printed or unprinted material or from the Internet have been cited according to the rules of good scientific practice and indicated by footnotes or other exact references to the original source.

The present thesis has not been submitted to another university for the award of an academic degree in this form. This thesis has been submitted in printed and electronic form. I hereby confirm that the content of the digital version is the same as in the printed version. I understand that the provision of incorrect information may have legal consequences.

(Signature)

(Place, Date)

ACKNOWLEDGEMENTS

I would like to thank all the people that have helped me during the thesis creation process. I am really grateful to my Supervisor for allowing me to work inside the group and for an opened chapter to fill the new information in. Further, I am truly thankful to Mr Maciej Chrzanowski, who have showed me the lab and instructed me with a great amount of technical knowledge, without which the thesis wouldn't have been done. Last but not least, I am indebted to the group of Prof. Ewa Popko, especially Dr. Piotr Biegański and Ms. Katarzyna Gwóźdź, for making many of the experiments and measurements available. To whom I did not include, thank you!

CONTENTS

List of Figures	9
List of Tables	11
1 INTRODUCTION	12
2 THEORY	15
2.1 CLASSICAL CONCEPTS OF LIGHT	15
2.1.1 ELECTROMAGNETIC FIELD	15
2.1.2 ENERGY OF ELECTROMAGNETIC FIELD, THE POYNTING VECTOR	17
2.2 PHYSICS AND PROPERTIES OF SOLIDS AND SEMICONDUCTORS	18
2.2.1 PHYSICS AND PROPERTIES OF SOLIDS	18
2.2.2 DRUDE MODEL OF FREE CARRIERS	19
2.2.3 CRYSTAL STRUCTURE AND BLOCH THEOREM	20
2.2.4 ENERGY STRUCTURE	21
2.2.5 BIGGER WORLD OF CARRIERS	22
2.2.6 NON-EQUILIBRIUM EFFECTS AND CARRIER INJECTION . .	25
2.2.7 SEMICONDUCTOR JUNCTIONS	26
2.3 LIGHT WITH MATTER INTERACTION	27
2.3.1 INTERBAND ABSORPTION	30
2.3.2 EXCITONS	31
2.3.3 PHOTOLUMINESCENCE	31
2.3.4 QUANTUM CONFINEMENT	33
2.4 PHOTOVOLTAIC DEVICES AND SOLAR CELL PARAMETERS	35
2.4.1 PROPERTIES OF SUNLIGHT	35
2.4.2 SOLAR CELL OPERATION	36
2.4.3 SOLAR CELL PARAMETERS	37
2.4.4 SHOCKLEY-QUEISSER LIMIT	38
2.4.5 EFFECTIVE RESISTANCE	39
2.5 QUANTUM DOTS AND QDSSC	40
2.5.1 SEMICONDUCTING QUANTUM DOTS	40
2.5.2 CORE-SHELL CQDS	41
2.5.3 CQD SUPER-CRYSTAL	41
2.5.4 PRINCIPLES OF QDSCS	42
2.5.5 MATERIALS AND PERFORMANCE DEVELOPMENT OF QDSSC - A REVIEW	43

3 PREPARATION, DEPOSITION AND OTHER EXPERIMENTAL METHODS	49
3.1 QUANTUM DOTS PURIFICATION	49
3.1.1 PURIFICATION METHOD	49
3.1.2 METHOD'S PROPERTIES	50
3.2 DEPOSITIONS PARAMETERS AND METHODS	50
3.2.1 GLASS CONTACT CLEANING	50
3.2.2 SPIN COATING	50
3.2.3 GLOVEBOX	51
3.2.4 SPUTTER DEPOSITION	52
4 RESULTS and Conclusion	53
4.1 PBS QUANTUM DOT SOLAR CELLS	53
4.1.1 PBS QUANTUM DOTS PRODUCED IN OUR LABORATORY .	54
4.1.2 FIRST DEVICE DEPOSITION	54
4.1.3 SECOND DEVICE MANUFACTURE	61
4.1.4 CONCLUSION AND OUTLOOK	68
5 FUTURE POSSIBILITIES	69
BIBLIOGRAPHY	69

LIST OF FIGURES

1.1	Energy sources contribution in world scale [33]	13
1.2	Annual yearly sum of Global Horizontal Irradiation [55]	14
2.1	Demonstrations of conductivity behaviour of different types of solids	19
2.2	The broadening of energy levels as atomic orbitals cross each other when they are getting closer[25]	21
2.3	Density of states behaviour[2]	23
2.4	Band diagram for intrinsic semiconductor and Fermi-Dirac function in $T > 0K$ - there is a possibility that electron will be excited to higher state [65]	24
2.5	For p-type material(right) we can excite valence band electrons into acceptor state easier so we have holes in the valence band and for n-type material(left) we can extract electrons from the donor level and have carries in the conduction band[3]	24
2.6	Band diagram for n type semiconductor when in equilibrium(left) and applying field(right)[65]	25
2.7	Schematics of space-charge distribution, electric field in the depleted region, potential distribution and energy structure of a p-n junction in thermal equilibrium	28
2.8	Image that shows the characteristic difference between two types of excitons. Wannier-Mott excitons are not constrained to any atom and can move freely through the material in contrast to the Frenkel excitons which are much less mobile[25]	31
2.9	Example of few of the processes that are present during photoluminescence[25]	32
2.10	Relaxation processes for excitons in the medium[65]	32
2.11	The image of a band structure for two band model in direct band semiconductors a). In b) we can see that there are much more discrete states in a nanoparticle than in bulk a) [46]	34
2.12	Quantum efficiency of an ideal silicon solar cell [4]	36
2.13	AM1.5 irradiation at Earth surface[5] and AM0 at Earth's orbit	39
2.14	Image of ideal CQD composed of selenide with passivation with oleic acid, oleyl amine and hydroxyl ligands [6]	40
2.15	Types of Core-Shell CQDs(blue color is core energy structure), we can see that in the first type both electrons(smallest energy in CB) and holes(biggest energy in VB) are confined beneath the core. [7]	41
2.16	Schematic illustration of configurations and band structures of QD solar cells: a) QD-sensitized b) hybrid QD-polymer c) Schottky junction d) p-n hetero-junction e) p-n homo-junction [35]	42
3.1	Cleaning methods environment	51

3.2	Laboratory equipment view	51
3.4	Sputtering deposition device that we were using	52
3.3	Sputtering deposition schematics(https://www.wikiwand.com/en/Sputter-deposition)	52
4.1	Emission spectrum of used PbS QDs [1]	53
4.2	Optical measurements of QDs synthesized by [77] and the procedure is described right there. It is worth to mention that the injection has been made at 80deg C. Graphs were included with kind acceptance of the former thesis author	55
4.4	First device and PbS Quantum-Dots produced in our laboratory	56
4.3	AFM picture of deposited ZnMgO layer b) and it's cross section a)	56
4.5	Comparison of Black Body photon counts and that of our light source	57
4.6	Original data from Gigahertz Optik GmbH	58
4.7	IV characteristics for QDSC and commercial cell	59
4.8	Laboratory absorption and photoluminescence measuring system	60
4.9	Energy structure of the first PbS-based QDSC	61
4.11	3D structure of the first device based on PbS QDs	62
4.10	Cell heating	62
4.12	Photoluminescence of purified QDs	63
4.13	Second deposition parameters and number of depositions made	63
4.14	Dark IV graph for the second device	64
4.15	First results from dark IV characteristics	65
4.16	Bright IV characteristics. Note that the destructed device characteristics is not used and the values displayed are for the first test	66
4.17	Power plotted for the first and second bright test. Maximal values of are plotted on the graph as well	66
4.18	Useful figure for bright characteristics of current density	67

LIST OF TABLES

4.1	Parameters of tested solar cells	59
4.2	PCEs of photovoltaic devices	59
4.3	Comparison of all of the solar cells	67

CHAPTER 1

INTRODUCTION

We, as a society nowadays, are in constant demand for energy. Although, even with the development of calculating, conducting and studying it, we don't really know what the energy is, we are depending on that abstract quantity. One might probably say that to study physics is to endure to study energy in its every possible form. There's a brilliant quote from Bill Bryson that: "Energy is liberated matter, matter is energy waiting to happen." What might be incredible is that from this strictly mathematical quantity we can deduct anything. And what's also important it is as arbitrary as it gets, depending only on one's reference. From energy we can create few more important quantities such as *power* P , which is simply the energy provided per unit time, so:

$$E = \int P(t) dt$$

The energy will be represented in J (Joules) or eV (electron volt), which directly describes energy of elementary charge ($e \approx 1.602 * 10^{-19} C$) in 1V (Volt) potential.

$$1eV = 1.602 * 10^{-19} J$$

Power will be then represented in W (Watts) ($W = \frac{J}{s}$).

The rise of energy consumption has proven that in the future we will almost certainly require even more. From Global Energy Perspective paper [39] we can learn that:

- Global energy demand will begin to reach a plateau at around 2035, despite a strong population expansion and economic growth, thanks to emphasis on renewable sources, more efficient service industries or more efficient industrial regions.
- The energy demand and economic growth has became "decoupled" for the first time in history.
- Renewable sources will provide more than half the electricity after 2035.

The reader is strongly recommended to take a look at the document.

With telling that we can produce energy there's a slick trick given with the phrase. Energy cannot be simply created, it is just converted from another source - so nothing is ever lost or miraculously made. The problems we need to struggle with are then being able to obtain as much energy from the energy source as it is possible. Of course, as humankind society is governed by money, we need to keep the cost lowest simultaneously. There is plenty of different energy sources, that we have learned of, to receive energy from. In Figure 1.1

we can see the most vivid ones nowadays. But with the human demand fulfilment come great damages and soon depleting resources of many energy sources such as fossil fuels.

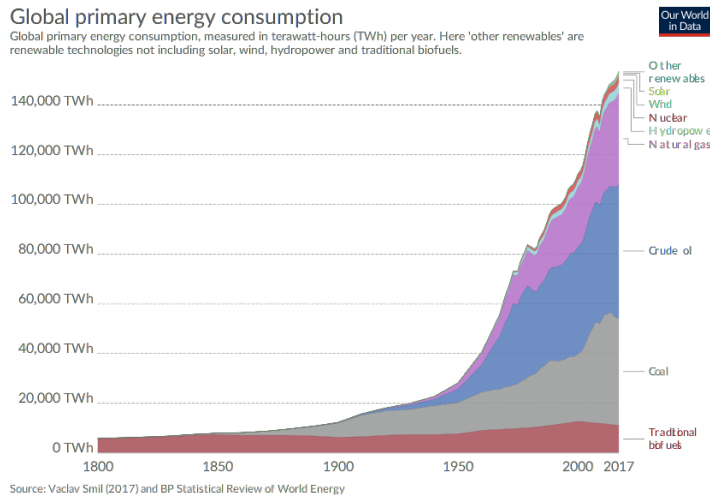


Figure 1.1: Energy sources contribution in world scale [33]

The necessity of searching new possible ways to harness it through renewable sources has become a global issue. Our concern of the environment had never been that serious before. Not only the change of methods for energy production must be enhanced because of this demand but we need to be strictly aware of the World's urging trepidation of Global Warming, of which evidence is provided for example here [59].

Among all of the ideas created in a past few decades, solar energy is believed by many to be one of the most reliable and promising. It can be directly converted into electricity, heat or chemical energy and our only Star seems to be an "infinite power" resource for us. In the last ten years the world solar PV electricity production has grown impressively, being almost three times bigger in 2016, than in 2010 [69]. In theory, the Sun has the potential to fulfil earth's energy demand, if it is not for the technology. Annually, nearly 10^{18} EJ of energy reaches our planet and of that 10^4 EJ is claimed to be harvestable[32]. The possibility of converting the solar energy into electric energy has been studied since discovery of the basic photovoltaic effect and the development of first semiconductor technologies.

Since the first crystalline silicon solar cell, the technology had undergone a vivid development. The number of different methods that the cell can be created with and the quantity of possible final outcomes isn't inconsiderable. Yet, solar cells can be classified into three generations in accordance to the development technology and materials used[35]. The first generation describes silicon based solar cells, which so far is the most researched type. It includes mono-crystalline and polycrystalline silicon cells.

The second generation contains thin film solar cells. It refers to amorphous silicon, copper indium gallium selenide (CIGS), GaAs and CdTe devices. With many advantages, such as direct band gaps resulting with harvesting light in very thin films, they still have a small share in the market of PV devices ($\approx 10\%$) due to their instability and limitation in module technology[35].

The third generation cannot be simplified as much as its formers. It is usually defined as solar cells that are still in scientific research phase[35] [18]. Its main motivation is to achieve a higher efficiency using newly discovered physical phenomena, structures and

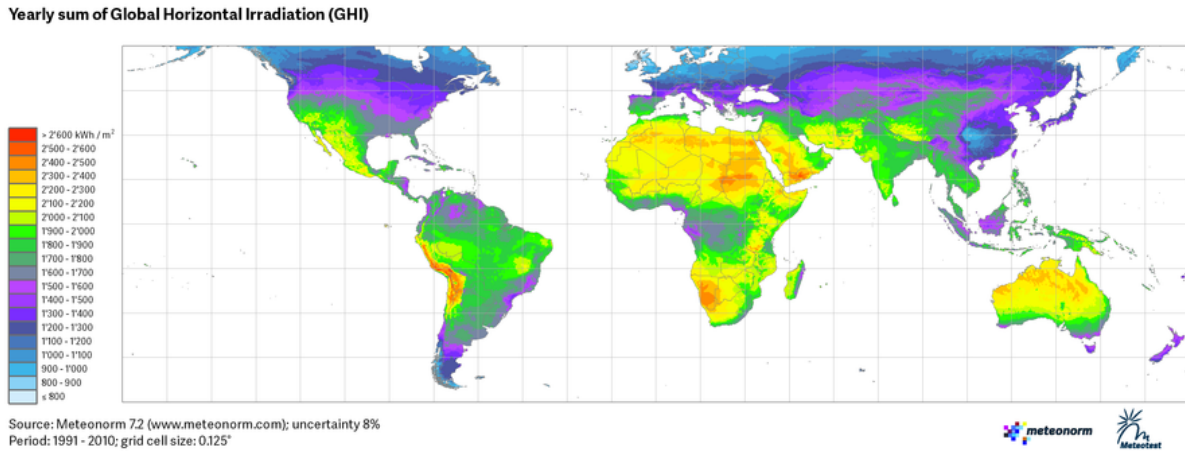


Figure 1.2: Annual yearly sum of Global Horizontal Irradiation [55]

materials. Their aim shall vary depending on the development technique and the physical principles. Today, the third generation mainly includes perovskite solar cells(PSCs) [15] [60], organic/polymer solar cells(OSCs) [23], dye sensitized solar cells(DSCs)[28] and quantum dot based solar cells(QDSC). [45] While still being considerably less common, the cons of investigating the nature and crucial properties of third generation PVs is overwhelming. Thanks to the ultimate specification of third generation approach, the devices can in perspective generate greater efficiency than other generations(for example by creating multiple electron-hole pairs and multi-band cells), yet while still being significantly cheaper than their formers.

Our main goal will be to study the QD sensitized solar cells and their characteristics. The base shall be put on PbS quantum dots as a light-harvesting material. We will proceed to consider their tunable band gap and other properties, such as control of composition, dipole moments, stability or collocation, and fit other materials to study the effects and their attributes. In principle, the QD solar cells can be distributed into four different classes: Schottky junction solar cells, p-n junction solar cells, hybrid QD-polymer solar cells and **quantum dot-sensitized solar cells (QDSCs)** and this is yet to be found later on...

CHAPTER 2

THEORY

With this chapter the introduction of some theoretical concepts will be provided. Certainly some of chapters below could be omitted without missing the final result and its meaning. Nevertheless, even if the paper is laced with rather practical analysis and effects, a physicist should be sure to understand the aspects of an experiment well, not just to have a better insight into the outcome but also to be sure that during the process no foolish mistakes are made and to be able to find new methods to improve the research. Therefore, few parts will just be a reminder and introduction to the used notation, or to ensure the understanding, and some will be treated as an inquiry of what might be searched to describe it further.

2.1 CLASSICAL CONCEPTS OF LIGHT

As in the photovoltaic physics we are constantly struggling with the light itself, we should know what the light actually is and how it interacts with matter in many, rather curious and different ways. Why is that so that matter looks the way it does and what of its properties can we control? In this chapter we will embrace the phenomena just to create an image of what we are dealing with.

2.1.1 ELECTROMAGNETIC FIELD

Before we actually begin we need to state some classic information about the physics of electric charges. The electromagnetic field is represented by two, generally complex, vectors, even though the physical result that we are expecting is ought to be real. Those vectors are **E** – *electric field* and **B** – *magnetic induction*. The properties of those fields are of course described by the *Maxwell's equations*. For them we shall also introduce two more important quantities ρ – *the electric charge density* and **j** – *electric current density* vector. We can define them in this way:

$$e = \int \rho dV \quad (2.1.1.1)$$

$$I = \int_S \mathbf{j} \cdot d\mathbf{S} \quad (2.1.1.2)$$

Where I is electric current.

The four Maxwell equations in differential form are:

$$\nabla \times \mathbf{E} = -\frac{\partial \mathbf{B}}{\partial t} \rightarrow \text{Faraday's induction law} \quad (2.1.1.3)$$

$$\nabla \times \mathbf{B} = \mu_0 \left(\mathbf{j} + \epsilon_0 \frac{\partial \mathbf{E}}{\partial t} \right) \rightarrow \text{Ampere's circuital law} \quad (2.1.1.4)$$

$$\nabla \cdot \mathbf{E} = \frac{\rho}{\epsilon_0} \rightarrow \text{Gauss's law} \quad (2.1.1.5)$$

$$\nabla \cdot \mathbf{B} = 0 \rightarrow \text{Gauss's law for magnetism} \quad (2.1.1.6)$$

To freely describe the properties of the fields interacting macroscopically with material objects we can also introduce standard auxiliary fields with polarization and magnetisation of a macroscopic medium. Those vectors are \mathbf{D} – *the electric displacement* and \mathbf{H} – *the magnetic vector*. From Gauss's law for magnetism there is a straight implication that no magnetics monopoles exist and Gauss's law may be also treated as electric charge density definition.

$$\mathbf{D}(\mathbf{r}, t) = \epsilon_0 \mathbf{E}(\mathbf{r}, t) + \mathbf{P}(\mathbf{r}, t) \quad (2.1.1.7)$$

$$\mathbf{H}(\mathbf{r}, t) = \frac{1}{\mu_0} \mathbf{B}(\mathbf{r}, t) - \mathbf{M}(\mathbf{r}, t) \quad (2.1.1.8)$$

Where \mathbf{P} is a *polarization vector* and \mathbf{M} is *magnetization vector*.

And with them our former equations change to:

$$\nabla \times \mathbf{E} = -\frac{\partial \mathbf{B}}{\partial t} \rightarrow \text{Faraday's induction law} \quad (2.1.1.9)$$

$$\nabla \times \mathbf{H} = \left(\mathbf{j} + \frac{\partial \mathbf{D}}{\partial t} \right) \rightarrow \text{Ampere's circuital law} \quad (2.1.1.10)$$

$$\nabla \cdot \mathbf{D} = \rho \rightarrow \text{Gauss's law} \quad (2.1.1.11)$$

$$\nabla \cdot \mathbf{B} = \mathbf{0} \rightarrow \text{Gauss's law for magnetism} \quad (2.1.1.12)$$

If we put divergence on the Ampere's law, we can then place Gauss's theorem in the equation because of the exchangeability of partial derivatives and from that we can simply derive so called equation for *charge conservation*:

$$\frac{\partial \rho}{\partial t} + \nabla \cdot \mathbf{j} = \mathbf{0} \quad (2.1.1.13)$$

The field is said to be static if all quantities are independent of time and, of course by itself, no currents are present. This is the special case, but we cannot be so lucky every time. Optical fields are usually sources of rapid time variety, but one may deal with it thanks to the possibility to average the field over macroscopic time interval which is mostly the case for photovoltaic needs, where for example the light source is at large distance. Relations for substances under influence of those fields can be considerably complicated. There is a special case that can make life easier as well. If the material is *isotropic* (all its properties are identical in every direction) they take a simple form of:

$$\mathbf{j} = \sigma \mathbf{E} \rightarrow \text{Ohm's law} \quad (2.1.1.14)$$

$$\mathbf{D} = \epsilon \mathbf{E} \quad (2.1.1.15)$$

$$\mathbf{B} = \mu \mathbf{H} \quad (2.1.1.16)$$

Here σ is called *conductivity*, ϵ is a *dielectric constant* and μ is *magnetic permeability*. Normally, all of those are tensors. In the case of scalar conductivity we can separate macroscopic media in three different categories: conductors, semiconductors and isolators. The same goes for magnetic permeability. With $\mu < 1$ the substance is said to be diamagnetic, $\mu > 1$ paramagnetic and so with $\mu \gg 1$ ferromagnetic. Obviously this description is rather intuitive and treated as a general theory. For example for exceptionally strong fields the area of non-linear optics is needed to be got into which provides higher power terms of fields in the above equations. Also, the case where we need to include relativistic effects by extracting previous values of \mathbf{E} acting on charges is not included as well. Of course, considering electromagnetic fields, we need to include the boundary conditions, yet they are not necessary for now. The information will be expanded later when needed, but if the reader wants to really expand following discussion understanding, it can be done via [13] [42].

2.1.2 ENERGY OF ELECTROMAGNETIC FIELD, THE POYNTING VECTOR

One might say that light is a transporter of energy itself, and the light intensity is easily interpreted as the energy flux of the electromagnetic field. All of the following equations can be beautifully derived via Lagrangian mathematics but we will just provide quick view derived from the Maxwell's equations.

From both Maxwell equations connecting rotations Eq.2.1.1.10 and Eq.2.1.1.9(they will be provided in CGI units now to show that we can use both) we can get:

$$\mathbf{E} \cdot \nabla \times \mathbf{H} - \mathbf{H} \times \nabla \times \mathbf{E} = \frac{4\pi}{c} \mathbf{j} \cdot \mathbf{E} + \frac{1}{c} \mathbf{E} \cdot \frac{\partial \mathbf{D}}{\partial t} + \frac{1}{c} \mathbf{H} \cdot \frac{\partial \mathbf{B}}{\partial t} \quad (2.1.2.1)$$

Then after using vector identities, integrating around some volume, using Gauss's theorem and introducing unit vector normal to the plane \mathbf{n} we get:

$$\frac{1}{4\pi} \int (\mathbf{E} \cdot \frac{\partial \mathbf{D}}{\partial t}) + (\mathbf{H} \cdot \frac{\partial \mathbf{B}}{\partial t}) dV + \int \mathbf{j} \cdot \mathbf{E} dV + \frac{c}{4\pi} \int (\mathbf{E} \times \mathbf{H}) \cdot \mathbf{n} dS = 0$$

Where the medium is thought to be isotropic. After taking material equations directly and introducing:

$$w_e = \frac{1}{8\pi} \mathbf{E} \cdot \mathbf{D} \quad (2.1.2.2)$$

$$w_m = \frac{1}{8\pi} \mathbf{H} \cdot \mathbf{B} \quad (2.1.2.3)$$

and

$$W = \int (w_e + w_m) dV \quad (2.1.2.4)$$

We now have:

$$\frac{dW}{dt} + \int \mathbf{j} \cdot \mathbf{E} dV + \frac{c}{4\pi} \int (\mathbf{E} \times \mathbf{H}) \cdot \mathbf{n} dS = 0$$

And W represents total energy contained in the arbitrary volume so therefore w_e and w_m are electric and magnetic energy densities respectively. From that after introducing total work needed to displace charges A we get:

$$\frac{dW}{dt} = -\frac{\delta A}{\delta t} - Q - \int \mathbf{S} \cdot \mathbf{n} dS$$

where Q is total charge and S is a Poynting vector interpreted as a density of energy flow and is equal:

$$\mathbf{S} = \frac{c}{4\pi} (\mathbf{E} \times \mathbf{H}) \quad (2.1.2.5)$$

2.2 PHYSICS AND PROPERTIES OF SOLIDS AND SEMICONDUCTORS

2.2.1 PHYSICS AND PROPERTIES OF SOLIDS

The most common distinction between solids is taking their resistivity as a criterion. We can distinguish three main categories for them - metals, semiconductors and isolators. Within that we can also provide temperature differences beneath them. As for the metals, the resistivity goes down with the temperature increase and for the rest of them it is quite the opposite.

Also, as it will be later extended, when we light a semiconductor or an isolator we can clearly observe so called *absorption threshold*. This is directly connected to the inner energy structure of a material(solutions to the Schroedinger equation and their restrictions).

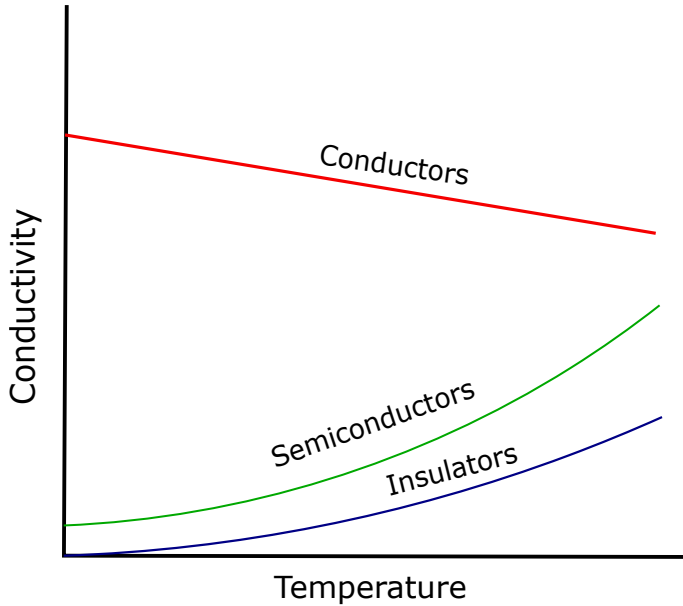


Figure 2.1: Demonstrations of conductivity behaviour of different types of solids

2.2.2 DRUDE MODEL OF FREE CARRIERS

The discovery of electron in 1897 had the great impact on the first attempt to describe properties of solids. Fairly early, just three years later, Drude constructed his first theory which based on the usage of quite successful kinetic theory, which described the behaviour of gases. Starting with metals, he imagined a gas of electrons which are identical solid spheres moving randomly in straight lines. They change directions by collisions and, of course, no other forces than that of the quick collisions are taken into account. As metals are neutral, Drude deduced that much heavier and steady particles are compensating negative electron charge. Strictly, that kind of model provides us with the crystal structure but back then, Drude assumed (and for great deal of metals it's fairly true), that only valence electrons are important and they move freely through the whole metal. The basic assumptions for the model are:

1. Between collisions, interactions electron-electron and electron-ion are able to be neglected. The first one is called *independent electron approximation* and the second is called *free electron approximation*.
2. Only the collisions are important. They are approximately instantaneous events and they significantly alter the velocity of the electron. The electron-electron scattering

is one of the least important scattering mechanisms in metals. Nevertheless with others, very often, in describing conducting electrons, it is not important to describe all mechanisms deeply.

3. We can assume that the period in which an electron isn't making any collision is τ (*relaxation time*) and thus the probability that electron is undergoing a collision in any infinitesimal time period dt is $\frac{dt}{\tau}$. This of course means that τ is average time and it is independent of both velocity and position → therefore also time.
4. Achieving thermal equilibrium is only through collisions.

ELECTRICAL CONDUCTIVITY

Drude model can describe, with certain accuracy, the Ohm's law $V = IR$. Resistance R is a quantity which is dependent of the dimensions of the material, therefore resistivity, which has been mentioned before can be used.

$$\mathbf{E} = \rho \mathbf{j} \quad (2.2.2.1)$$

The current density j is the same as in former section, when we were describing Maxwell's equations. If n electrons move with velocity \mathbf{v} in time period dt and through area A we get that charge connected with that quantities is $-nevAdt$ so current density is:

$$\mathbf{j} = -nev \mathbf{v} \quad (2.2.2.2)$$

and is just a net current because of random electron movement. Also, let's assume that electron has a velocity \mathbf{v}_0 at time t_0 just after a collision and additional velocity $\frac{-\mathbf{E}e\tau}{m}$ provided by the presence of an external field, we can take average through long time period. The random velocity \mathbf{v}_0 disappears and therefore, connecting with 2.2.2.2 we get that:

$$\mathbf{j} = \sigma \mathbf{E} \quad (2.2.2.3)$$

$$\sigma = \frac{ne^2\tau}{m} \quad (2.2.2.4)$$

This tells us about the linear dependence of \mathbf{j} on \mathbf{E} . Note that $\tau = \frac{m}{\rho n e^2}$ because $\tau = 1/\rho$ where ρ is *resistivity*. Drude model was a first and simple model used in describing solid state materials. As simple as it is, it can yet provide some accurate results. Even more can be read in [58]

2.2.3 CRYSTAL STRUCTURE AND BLOCH THEOREM

To easily get to quantum dot description, we shall know that most materials used nowadays occur as crystals. They possess a so called translational order, which can be described by **Bloch theorem** and is a point group symmetry. The symmetry has its impact on most physical properties of a material, therefore it is important to study if a material possesses crystal symmetries.

The Bloch theorem simply says that electron in a periodic potential $V(\mathbf{r})$ can be described as

$$\psi_{\mathbf{k}}(\mathbf{r}) = u_{\mathbf{k}}(\mathbf{r})e^{i\mathbf{k}\mathbf{r}} \quad (2.2.3.1)$$

where \mathbf{k} is a wave vector and $u_{\mathbf{k}}$ has a periodicity of a crystal lattice so $u_{\mathbf{k}}(\mathbf{r}) = u_{\mathbf{k}}(\mathbf{r} + \mathbf{R}_n)$ and \mathbf{R}_n is an arbitrary lattice vector. The lowering of symmetry can provide optical anisotropy(optical properties are different in different directions) and lift degeneracies(provide more possible energy states in a system). Anisotropy is only found in solids.

2.2.4 ENERGY STRUCTURE

Bloch theorem 2.2.3.1 tells us more about a form of a wavefunction. It also describes each electronic band(the effect of mixing atomic orbitals which provides the broadening in a discrete energy levels into so called bands).

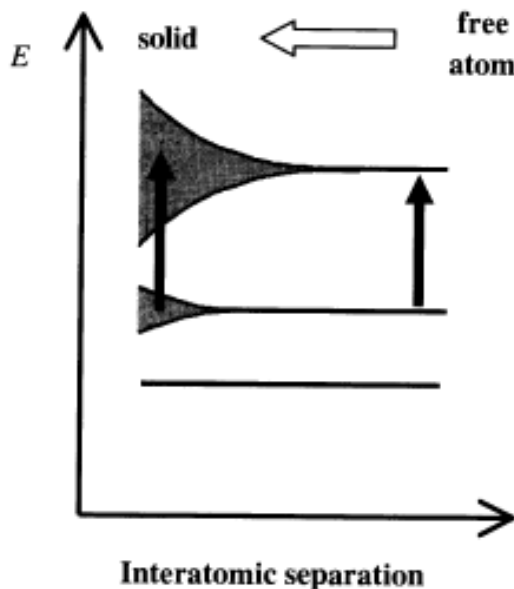


Figure 2.2: The broadening of energy levels as atomic orbitals cross each other when they are getting closer[25]

Optical transitions that are possible for distinct material and are available via *selection rules*, occur between each electronic band, of course if the beginning state is occupied and ending is empty. This *absorption* is possible over a range of energies that are bigger than the gap between those levels. The energy structure is also widened because of the vibration bands that are possible because of the coupling between continuum of vibrational modes of the crystal and those electronic bands. What is important, those effects are also present in molecular materials such as QDs.

With the term of band formation, we cannot omit **the density of states**. It gives us the number of states that is possible to achieve in an abstract range of energies.

$$\text{number of states in } [E, E + dE] = g(E)dE$$

and is usually obtained from $E(\mathbf{k})$ dependence

$$g(E) = g(k) \frac{dk}{dt} \quad (2.2.4.1)$$

2.2.5 BIGGER WORLD OF CARRIERS

In reality of course, we cannot describe the carriers in the medium with such smooth potential like in metallic models. The potential periodicity that comes from the crystal periodicity gives us important informations about the behaviour of the electrons. The set of possible energies of an electron in periodic potential is quadratic $E = \frac{\hbar^2 k^2}{2m_e}$. Also, in consequence of the Bloch law, being directly evaluated from the Schrödinger equation we have that:

$$\Psi_{n,\mathbf{k}}(\mathbf{r}) = \Psi_{n,\mathbf{k}+\mathbf{G}}(\mathbf{r}) \quad (2.2.5.1)$$

$$E_n(\mathbf{k}) = E_n(\mathbf{k} + \mathbf{G}) \quad (2.2.5.2)$$

where \mathbf{G} is a *Reciprocal lattice vector*.

$$\mathbf{G} = n_1 \mathbf{b}_1 + n_2 \mathbf{b}_2 + n_3 \mathbf{b}_3 \quad (2.2.5.3)$$

The periodicity of a crystal allows also to create *The first Brillouin zone* which preserves that symmetry. We can also say that the number of available wavevectors in the I Brillouin zone is equal to the number of the primitive cells in the crystal volume (the cells that with translation can reproduce the whole crystal) (this also means that one cell gives one possible \mathbf{k} state, so we have $2N$ possible states when considering electron spin).

The electric current can flow through the body, if the band isn't fully occupied by electrons. So we can say that transport properties are indicated by the last electronic band, called *Conduction band*. To describe distinct potentials much easier it is usual to provide the concept of effective mass of a carrier in a band.

$$m_e^* = \left(\frac{1}{\hbar^2} \frac{d^2 E}{dk^2} \right) \quad (2.2.5.4)$$

and is a tensor in three dimensions. It can be noted that in the minimum of conduction band the effective mass is almost equal to the mass of a free electron. With that concept there comes another simple idea as well. Instead of using electrons in a band that's almost fully occupied (*the Valence band*) we can use the imaginary carriers - holes, which are the vacancies of an electron. To do it, we have to put it's mass and charge to be negative $m_p^* = -m_e^*$ and it's momentum $k_p = -k_e$. So now we have energy of an electron in conduction band:

$$E(k) = E_c + \frac{\hbar^2 k^2}{2m_e} \quad (2.2.5.5)$$

and energy of a hole in valence band:

$$E(k) = E_v + \frac{\hbar^2 k^2}{2m_p} \quad (2.2.5.6)$$

After saying that, to calculate the concentration of carriers in thermodynamic equilibrium we have to consider the yet introduced *density of states* $g(E)$ and the probability that the state will become occupied - *the Fermi-Dirac function* $f(E)$. For electrons:

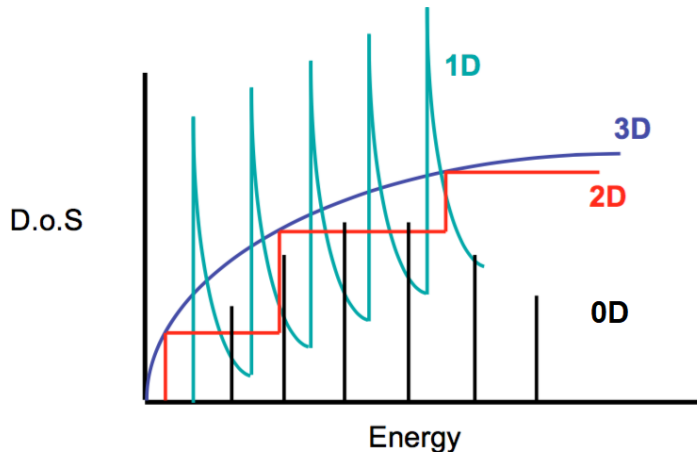


Figure 2.3: Density of states behaviour[2]

$$n_0 = \int_{E_c}^{\infty} f(E)N(E)dE \quad (2.2.5.7)$$

Because of the difficulty and the complexity of $g(E)$ it is usually calculated numerically. Few facts can be said before though:

- inside the band gap $g(E) = 0$
- in three dimensions $g(E) \propto \sqrt{E - E_c}$
- inside the band $g(E)$ is non-analytic(infinities from the derivative - Van Hove singularities)

Here, we will also state the Fermi-Dirac distribution function:

$$\frac{1}{1 + e^{(E_c - E_F(T=0K))/kT}} \quad (2.2.5.8)$$

Where E_F is a Fermi level - the highest possible energy for electrons to posses at absolute zero temperature, (also chemical potential). Very often in intrinsic semiconductors it is called E_i .

In intrinsic semiconductors(without any impurities) number of electrons in conduction band is equal to the number of holes in valence band because the electron excitation leaves exactly one vacancy behind. It is illustrated in Fig. 2.4

In all semiconductors in thermal equilibrium we have:

$$n_0 p_0 = n_i^2 \quad (2.2.5.9)$$

The concept of an intrinsic semiconductor is rather idealistic, so in reality the crystal of a semiconductors has defects, intentional or not. We can have donor(more electrons than original atom) and acceptor(less electrons than original atom) impurities so there can another donor or acceptor energy levels be created for carriers to jump easier into. For type n semiconductor, the current flow is mostly due to electrons and for type p due to holes.

As a result of the placement of Fermi level in non-intrinsic semiconductors, when comparing with the Fermi level of an intrinsic one, the equilibrium concentration is:

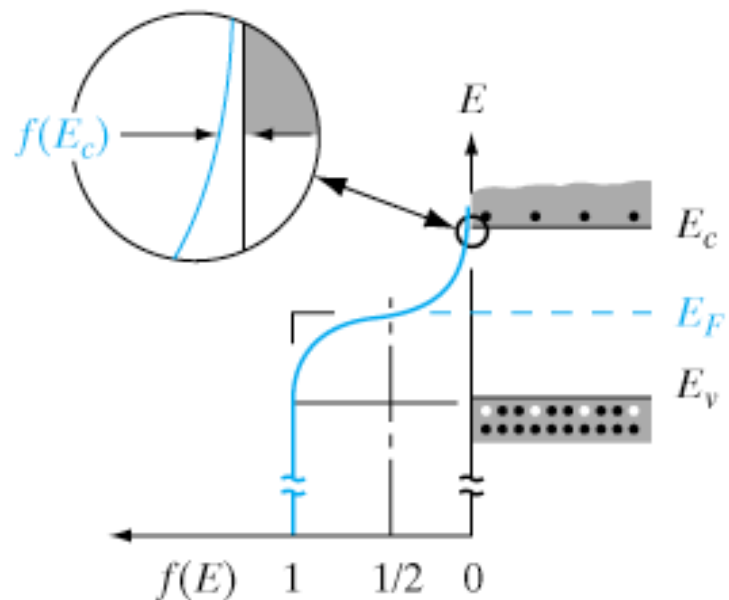


Figure 2.4: Band diagram for intrinsic semiconductor and Fermi-Dirac function in $T > 0K$
- there is a possibility that electron will be excited to higher state [65]

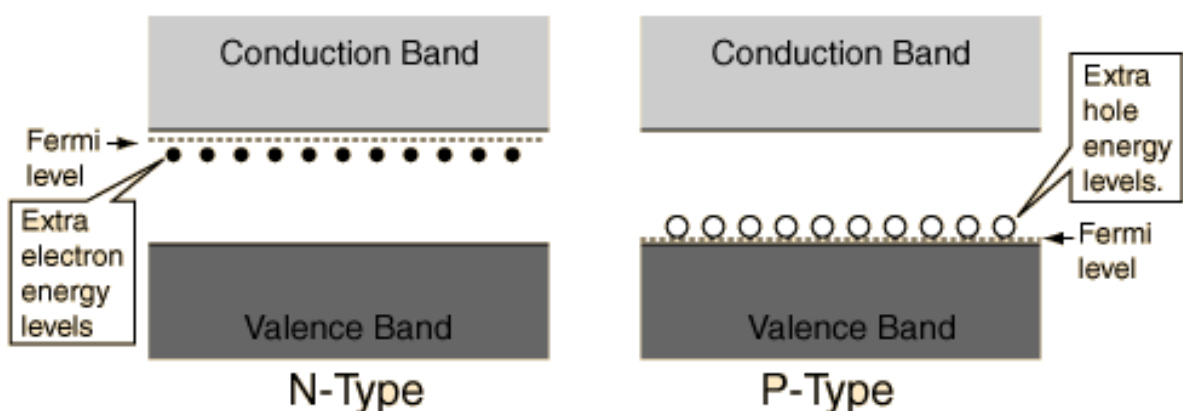


Figure 2.5: For p-type material(right) we can excite valence band electrons into acceptor state easier so we have holes in the valence band and for n-type material(left) we can extract electrons from the donor level and have carries in the conduction band[3]

$$n_0 = n_i e^{(E_F - E_i)/kT} \quad (2.2.5.10)$$

$$p_0 = p_i e^{(E_i - E_F)/kT} \quad (2.2.5.11)$$

2.2.6 NON-EQUILIBRIUM EFFECTS AND CARRIER INJECTION

In all semiconductor physics most phenomena are based on non-equilibrium effects. With the chaotic thermal movement of the carriers, there's also effect of applying electric field to the semiconducting sample. The chaos of course cancels all components of the currents so no net mean velocity is present. The resulting current is therefore only the effect of applied field and is described using quantity called **carrier mobility** $\mu = \frac{\langle v \rangle}{\epsilon}$. Where ϵ is the electric field and $\langle v \rangle$ is the average velocity. When also including holes in the transport we get:

$$\mathbf{J} = q(n\mu_e + p\mu_p)\epsilon \quad (2.2.6.1)$$

where q is the electric charge and n, p are electron and holes concentrations respectively. Application of the electric field also changes the band diagram of the structure. Let's say we put electric field in the x direction. Then the force is equal:

$$F = -q\epsilon = -\nabla E_p \quad (2.2.6.2)$$

where E_p is the potential energy in this conservative field. Then:

$$\epsilon = \frac{1}{q} \frac{dE_p}{dx} \equiv -\frac{dV}{dx} \quad (2.2.6.3)$$

and V is the electric field potential.

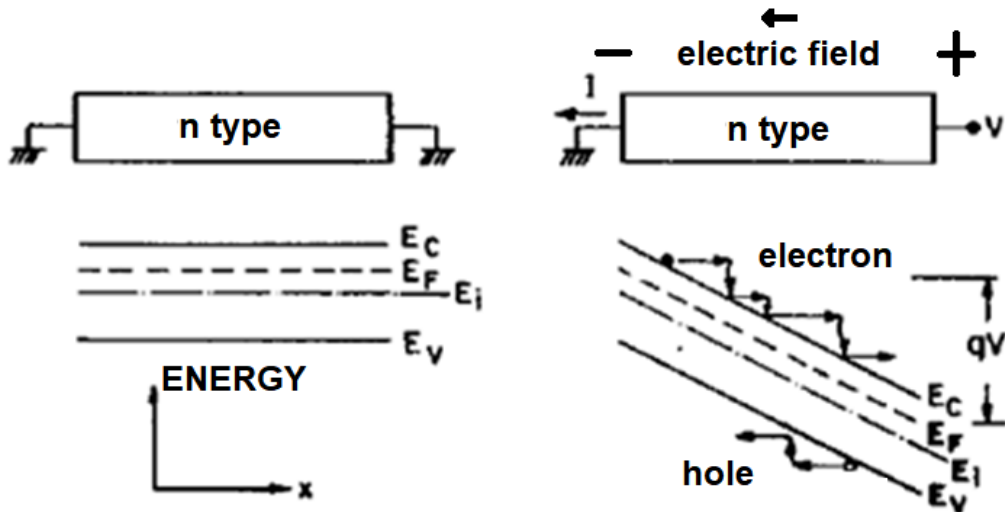


Figure 2.6: Band diagram for n type semiconductor when in equilibrium(left) and applying field(right)[65]

If the concentration changes, the uniformity isn't preserved. Then, the gradient of a concentration creates its own current. It is called the *diffusion current* and is equal:

$$J_{n_{diff}} + J_{p_{diff}} = qD_e \frac{dn(x)}{dx} - qD_p \frac{dp(x)}{dx} \quad (2.2.6.4)$$

$D_{n(p)}$ is a diffusion coefficient and is connected to the mobility via Einstein equation so that: $D_{n(p)} = \mu_{n(p)} kT/q$. Notice both that holes and electrons move in the other direction the concentration gradient, but because of the negative value of electron charge both of currents are in the opposite directions.

Carrier injection is connected to the situation where the excessive carriers are created in order of applying electric field or applying light on a sample. Then $np \geq n_i^2$. After the injection process, there occurs an undesirable effect in the photovoltaic physics - **recombination**.

We can say that there are three processes of recombination in the bulk:

- Radiative(interband) recombination - electron loses energy by emitting photon with wavelength similar to the energy difference between bands.
- Defect levels - Shockley-Read-Hall recombination. Electron or hole can be either trapped in additional defect energy state inside the band gap or if the carrier jumps to the energy state before thermal re-emission occurs.
- Auger recombination - involves extra two carriers, when recombination of one hole and one electron produces energy to excite third carrier higher in the band.

More about recombination will be said concerning quantum dots.[65] [4]

QUASI-FERMI LEVELS

It is worth to be noted now, that when in equilibrium the thermal generation of carriers is compensated by the recombination processes so equilibrium concentrations of both electrons and holes don't change on their own. The situation changes drastically, when we provide the light source to create the light-induced carrier generation. Then, concentrations n and p will increase. Providing that excessive concentrations for holes and electrons are the same(no traps are included), we can calculate the non-equilibrium carrier concentrations as:

$$n = n_i e^{(F_n - E_i)/kT} \quad (2.2.6.5)$$

$$p = n_i e^{(E_i - F_p)/kT} \quad (2.2.6.6)$$

where F_n and F_p are quasi-Fermi levels of electrons and holes respectively. Their shift from E_F , induced by excessive carriers, is the way to distinguish how the equilibrium concentrations have changed.

2.2.7 SEMICONDUCTOR JUNCTIONS

After stating previous information, let's imagine now that we connect two semiconducting materials together(no matter what technique with). Both of them have its own Fermi level. Then, after connecting them, the Fermi level gradient becomes $\frac{dE_F}{dx} = 0$. If, additionally, we provide the non-equilibrium process, such us electric field or light induced carrier injection, the quasi-Fermi levels gradients become non-zero. For electron current only,

induced with gradient concentration and electric field polarisation in the x direction we get:

$$J_n(x) = q\mu_n n(x)\epsilon(x) + qD_n \frac{dn(x)}{dx} \quad (2.2.7.1)$$

Then after taking the excessive concentrations with quasi-Fermi levels included we get:

$$J_n(x) = \frac{\sigma_n(x)}{q} \frac{dF_n}{dx} \quad (2.2.7.2)$$

where we can see that net current is strictly connected with the gradient of quasi-Fermi level. (Same can be done for holes)

P-N JUNCTION

A quick insight into p-n junction physics shall be put as it is in the principles of photovoltaic physics. Nevertheless, it would be just a reminder to the concept and more information can be obtained from f.e [78] After connecting two semiconductors together, we know that for the equilibrium to be conserved our Fermi level gradient has to be 0 through the sample. This creates the difference in the energy structure which is called the built-in potential $\Phi_{bi} = \Phi_n - \Phi_p$ (because both of the Fermi levels must adjust to each other), where $\Phi_{n,p}$ is potential connected with the n or p type semiconductors respectively. For this to occur, because of the concentrations gradient between both materials, some of the electrons must go to the p type semiconductor, leaving volumetric positive charge behind. The holes from the p type "behave" the same way. This also explains the built in potential and creates the electric field between two sides called the **depletion region**. Because of the equilibrium $n_{n0}p_{n0} = n_{p0}p_{p0}n_i^2$ (the first letter states the side of the sample) we can calculate the built in potential by using the concentration with:

$$\Psi_{bi} = \frac{kT}{q} \ln\left(\frac{p_{p0}}{p_{n0}}\right) = \frac{kT}{q} \ln\left(\frac{n_{n0}}{n_{p0}}\right) \quad (2.2.7.3)$$

The width of a depleted region, the sizes for n and p types and potential distribution inside are usually calculated by assuming the box shape of the region. Because the electric field far from the junction must be zero, the total negative electric charge density, which was created in p-type, must be equal to positive charge density in the n type. Therefore we can say that:

$$N_A W_p = N_D W_n \quad (2.2.7.4)$$

where $N_{A,D}$ are acceptor and donor atoms concentrations and $W_{p,n}$ are lengths of box-approximated parts of the depleted region for p and n typ, see Fig.(2.7). From Poisson equation we can calculate further each of the quantities [78].

From that all we can derive the Shockley diode equation for the total current density[4]

$$J = J_0(e^{\frac{qV}{kT}} - 1) - J_{sc} \quad (2.2.7.5)$$

2.3 LIGHT WITH MATTER INTERACTION

From the wide set of examples of how the light can interact with matter in principle, the generalisation can be provided to create a distinction of three groups - reflection,

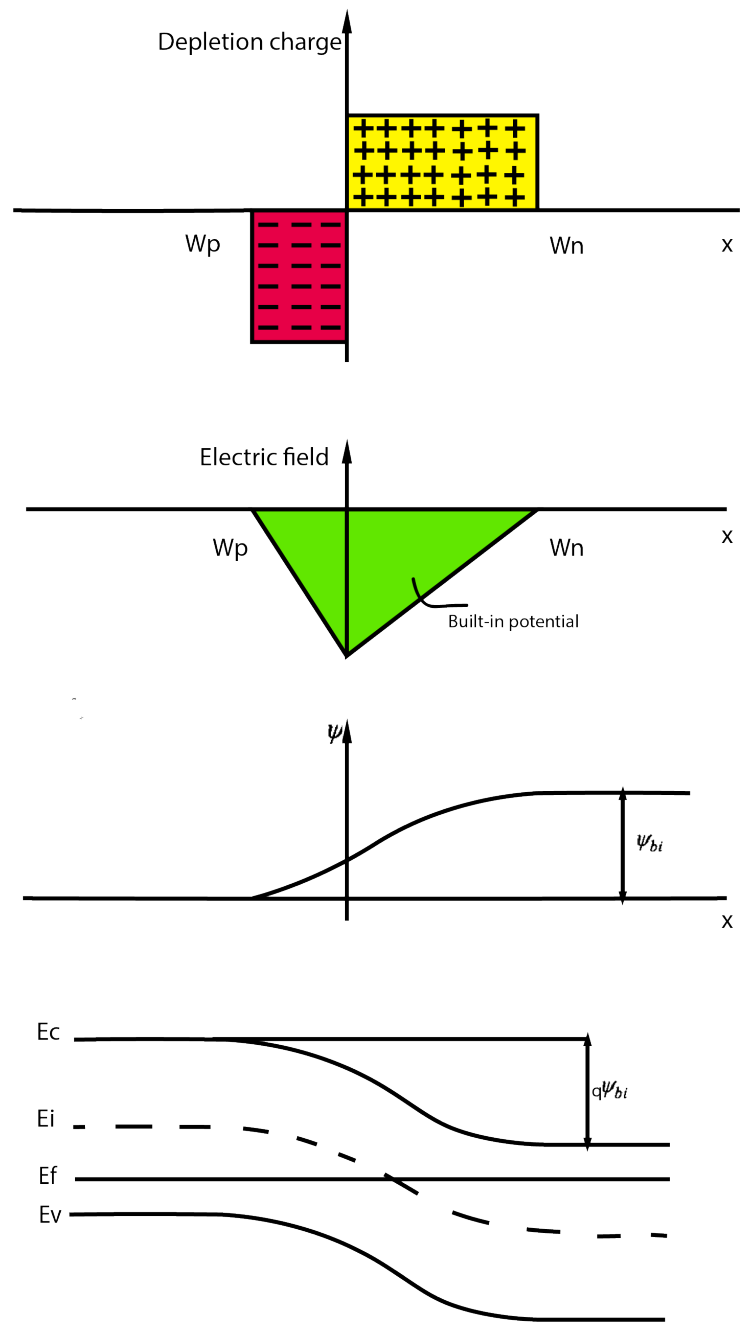


Figure 2.7: Schematics of space-charge distribution, electric field in the depleted region, potential distribution and energy structure of a p-n junction in thermal equilibrium

propagation and transmittance. During its propagation in the body, the light can be:

- Refracted - bends of the light ray when inside the medium which cause the macroscopic effect in changing the light velocity when compared to the open space.
- Absorbed - as has been said before, it occurs when we have the resonant frequency of the light to provide a transition of a particle to the higher possible energy level.
- Emitted with luminescence process- is connected to the spontaneous emission but is not always provided after an absorption. The light emitted from the medium is in all directions and has different frequency than incident light(this is called the Stokes shift and will be explained later), if the absorption is its former inductor.
- Scattered - this changes the direction and sometimes the frequency of the input light. This is caused by the tiny changes of the frequency at the wavelength length scale. If the scale of the scattering centres are significantly smaller than the wavelength then we have the situation of the **Rayleigh scattering**.

It is also worth to note the refractive index of the medium as the change ratio of velocity in free space to velocity in the medium $n = \frac{c}{v}$. It's dispersion relation(connection to the frequency of the light) is directly connected to the inner processes that will be stated later on.

Absorption inside the medium is also macroscopically described by the **Beer's law**. It creates a description as fraction of power that is absorbed by the unit length of the sample and has its exponential form of:

$$I(z) = I_0 e^{-\alpha z} \quad (2.3.0.1)$$

where light propagates in the z direction, I_0 is intensity of the light at $z = 0$ and α is the absorption coefficient(which also has the dispersion relation). This can be even extended when generalised to the complex refractive index.

$$\tilde{n} = n + i\kappa \quad (2.3.0.2)$$

where n is the normal refractive index and κ is an extinction coefficient and is directly connected to the α coefficient. Generalization of the wave vector \mathbf{k} is

$$k = \tilde{n} \frac{\omega}{c} \quad (2.3.0.3)$$

so with the Beer's law we have that electric field is(because $I \propto$ square root of the electric field module):

$$\varepsilon(z, t) = \varepsilon_0 e^{\kappa \omega z / c} e^{i(\omega nz / c - \omega t)} \quad (2.3.0.4)$$

So extinction coefficient isn't connected to the phase, but to the exponential decay. We also usually provide **complex relative dielectric constant** ε_r

2.3.1 INTERBAND ABSORPTION

The fact that the semiconductors have the fundamental band gap creates a hard absorption edge in the spectra. The excitation between bands provide transitions for the certain range and leads to different processes later. The classical model of oscillatory electronic vibrations fails to deal with the discrete states, as they are in the media, therefore we need to apply some quantum mechanics to provide the reliable description as we are dealing with nanostructures. Like we said before, the difference between bands is the band gap E_g . Transitions between them are only possible when selection rules allow them and the frequency is fitted to it. If there is an electron possible to be excited we also need to fulfil the **Pauli exclusion principle** that states that the higher state must be empty. Let's say that the initial energy is E_i and the electron is excited with a photon to the final energy E_f above the band gap. This creates an electron-hole pair.

$$E_f = E_i + \hbar\omega \quad (2.3.1.1)$$

The band gap in semiconductors can be *direct* or *indirect*. The first case is when the maximum of the valence band and minimum of the conduction band is at the wavenumber $\mathbf{k} = 0$. The second case is when conduction band minimum is moved at the different \mathbf{k} . The transition rate from the initial state to the final state is provided by the **Fermi's Golden Rule**:

$$W_{i \rightarrow f} = \frac{2\pi}{\hbar} |M|^2 g(\hbar\omega) \quad (2.3.1.2)$$

where M is the transition matrix element and $g(\hbar\omega)$ is again the density of states. The first one is just the element of the Hamiltonian.

$$M = \langle f | H' | i \rangle = \int \psi_f^*(\mathbf{r}) H'(\mathbf{r}) \psi_i(\mathbf{r}) d^3r \quad (2.3.1.3)$$

of course, H' is not the standard Hamiltonian but the external-perturbation-induced and is connected to the incident light wave. With semiclassical model, where we don't quantize the electromagnetic wave but just electrons, we have(using the electron **dipole moment** \mathbf{d}):

$$H' = -\mathbf{d} \cdot \varepsilon_{photon} \quad (2.3.1.4)$$

where

$$\varepsilon_{photon}(\mathbf{r}) = \varepsilon_0 e^{\pm i\mathbf{k} \cdot \mathbf{r}} \quad (2.3.1.5)$$

To finish the calculation it is important to input the wavefunction of an electron but we will just state the conservation of momentum, as the standard Bloch theorem works only for crystalline solids. It is crucial that the change of electron momentum must be equal to the photon momentum so:

$$\hbar\mathbf{k}_f - \hbar\mathbf{k}_i = \pm \hbar\mathbf{k} \quad (2.3.1.6)$$

For the indirect band materials, to conserve the momentum, we need to add emission or absorption of a phonon, which changes the light absorption dependence.

2.3.2 EXCITONS

Leaving the electron-hole pair in different bands provides a possibility of the mutual Coulomb interaction between them. This is an attractive interaction which possesses a very unique properties.

Exciton can be considered as a small hydrogen like system. Two basic types of them are observed:

- Wannier-Mott excitons - free excitons
- Frenkel excitons - tightly bound excitons

For their size, the Frenkel excitons are more probable to be found in molecular materials and nanostructures.

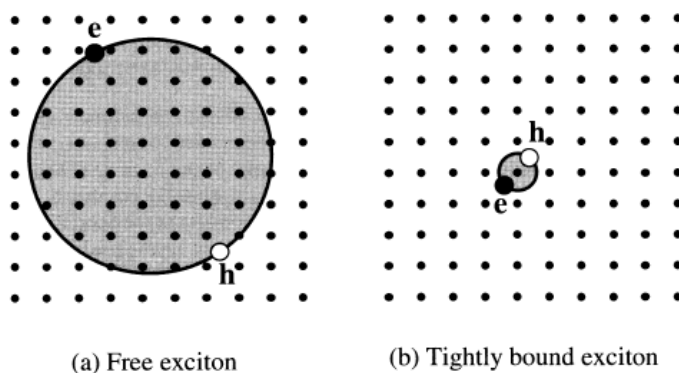


Figure 2.8: Image that shows the characteristic difference between two types of excitons. Wannier-Mott excitons are not constrained to any atom and can move freely through the material in contrast to the Frenkel excitons which are much less mobile[25]

Stability of the exciton is strictly induced with the possibility of their potential to be big enough not to allow collisions with phonons.

2.3.3 PHOTOLUMINESCENCE

Photoluminescence may be described as an emitted electromagnetic radiation being a result of it's former excitation. The excited state depends on the internal energy structure of a radiated object and is an unique example of non equilibrium state. We might say from now on that during the whole luminescence process three possible scenarios are to be observed.

- Firstly the electron-hole pair is created.
- The recombination process occurs.
- Then the radiation escapes from our sample.

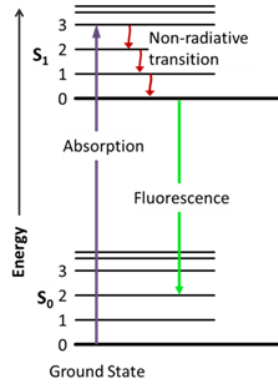


Figure 2.9: Example of few of the processes that are present during photoluminescence[25]

The recombination is most probable near the surface of the sample, therefore the depletion of the carries is possible starting with the recombination processes which can be both radiative or non-radiative. Following that the recombination radiation is most usually emitted near the surface again, the great amount of experiments are created in the manner to directly look into the irradiated side.

The thing that luminescence can be in the same time as the absorption doesn't change the fact that it is quite different than it. In luminescence atoms emit light via the spontaneous emission so it's indivisibly defined by all of the vast majority of relaxation processes. The luminescence is divided into photoluminescence and electroluminescence. We can use it to study the band gaps, transitions from it or transitions from deep doping states and defects. From the PL we can extract such informations as types and concentration of doping. Then, as we change the sample temperature, we can also see how many relaxing centres are realised inside the medium. The possible relaxation types for exciton are shown in [Figure 2.10]

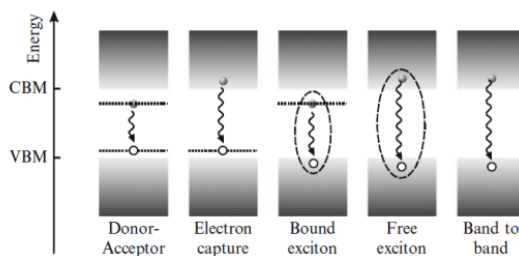


Figure 2.10: Relaxation processes for excitons in the medium[65]

To describe spontaneous emission we can use Einstein A coefficient which is directly connected with B coefficient responsible for absorption and is different for different materials. This can be derived directly from Quantum Optics. When we have upper level populated at N at a time t we can say that:

$$\left(\frac{dN}{dt} \right) = -AN \quad (2.3.3.1)$$

This tells us that emission behaves exponentially with τ_R being the radiative lifetime of a transition. The relaxation not always goes with photon emission, there can be a non-

radiative one as well(f.e. as heat by creating lattice vibrations called phonons) and this is restricted by comparing the time-scales of emissions.

2.3.4 QUANTUM CONFINEMENT

The properties of small systems are obviously rather different than those of a bulk. The confinement in those kind of structures plays a crucial role in describing their physical properties. The first idea to describe semiconductors using quantum confinement and quantum mechanics methods has been used by Esaki and Tsu in 1970 [22], which has led to extreme advancement in describing the phenomena semiconductor physics. All things that are connected to optical properties of confined structures are directly derived from all the things that are connected to optical properties of solids described above.

Changing the size of the crystal leads to great difference in the optical properties. The confinement effect in tiny regime leads us to the **Heisenberg uncertainty principle**, which tells us that the more we know the position of an object Δx , the less we know its momentum Δp_x

$$\Delta x \Delta p_x \geq \frac{\hbar}{4} \quad (2.3.4.1)$$

This confinement leads to additional term to kinetic energy of particle with mass m connected to the uncertainty of momentum:

$$E_{con} = \frac{(\Delta p_x)^2}{2m} \quad (2.3.4.2)$$

This energy can play an important part in it's energy when it is comparable or greater than the thermal kinetic energy, which, let's say, on average is $\frac{1}{2}k_B T$. This tells us that quantum effect will be considerable if the determined position is the size of $\sqrt{\frac{\hbar^2}{mk_b T}}$. This can be transformed and stated that the position must be in the order of the **de Broglie** wavelength of an object $\lambda_{dB} \equiv \frac{p_x}{\hbar}$.

Quantum confined structures are classified by the dimensions they are confined in.

- Quantum wells(confinement in 1-D)
- Quantum wires(confinement in 2-D)
- **Quantum dots**(confinement in 3-D)

The confinement of carriers in quantum dots describes that the carriers are completely localised on the particle. To describe the three dimensional confinement, the model of the particle in a box has been used as a first method to the problem. Later on, it has been extended with more terms in the Hamiltonian like Coulomb interaction or non-parabolic and more complicated band structures. Those models have given rise to new properties such as: selection rules, radial wavefunction shape and the energy structures. This has shown that to truly understand the phenomena, we need to use non-linear optics as well. The beginning consists of going through one electron-hole pair(1EHP) states and then increasing the population and density of excited states by f.e differing the size of the nanoparticle. We will now state the 1EHP theory results and tell where can it can be further explained.

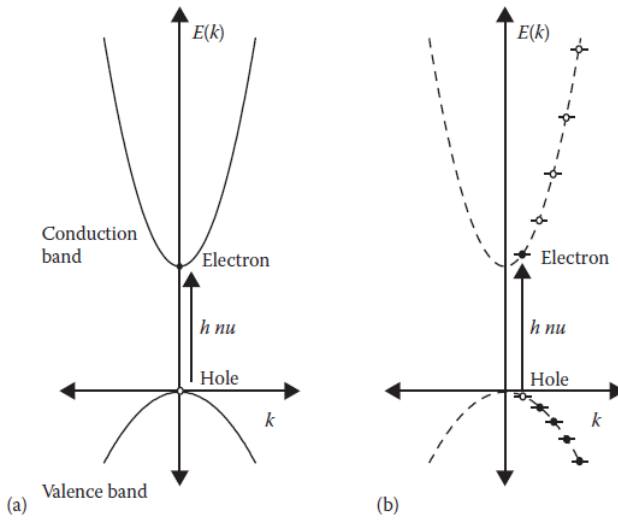


Figure 2.11: The image of a band structure for two band model in direct band semiconductors a). In b) we can see that there are much more discrete states in a nanoparticle than in bulk a) [46]

THE PARTICLE IN A BOX

This model is used in describing a behaviour of a particle with mass m in a spherical potential with radius a . [46]

$$V(r) = \begin{cases} 0 & r < a \\ \infty & r \geq a \end{cases}$$

where the radius can differ for holes and electron. This type of potential is connected with solving the stationary Schroedinger equation:

$$\hat{H}\Psi(\mathbf{r}) = E\Psi(\mathbf{r}) \quad (2.3.4.3)$$

The potential containing the semiconductor sphere is relatively infinitely high. In that kind of environment, the wavefunction is a product of a Bloch function and a new envelope function. The periodic Bloch part shall be the same in the barrier and the well.

$$u_k(r)_{\text{barrier}} = u_k(r)_{\text{well}} = u_k(r) \quad (2.3.4.4)$$

The whole function now:

$$\Psi(r) = \psi(r)u_k(r) \quad (2.3.4.5)$$

where $\psi(r)$ is the new envelope function for electrons and holes. We now have that(neglecting the other interactions - in single parabolic band approximation):

$$\hat{H} = \left[\frac{-\hbar^2}{2m_e} \nabla_e^2 + \frac{-\hbar^2}{2m_h} \nabla_h^2 \right] + V_e(\mathbf{r}) + V_h(\mathbf{r}) = \quad (2.3.4.6)$$

The envelope function is separable for holes and electrons so the solutions have a shape like:

$$\Phi_{nlm}^i(r) = Y_{lm} \sqrt{\frac{2}{R^3}} \frac{J_l(\chi_{nl} \frac{r}{R})}{J_{l+1}(\chi_{nl})} \quad (2.3.4.7)$$

where $-l \leq m \leq l; l = 0, 1, 2, 3, \dots; n = 1, 2, 3, \dots$, Y_{lm} are spherical harmonics and J_l are the Bessel functions and χ_{nl} is the n -th zero of order 1 Bessel function. When we put effective masses we can estimate roots and calculate the energy levels for the envelope functions. Then we can calculate the optical properties calculating the overlap of the functions. Nevertheless, this approximation cannot fully explain what happens with the nanoparticles. We have simply neglected all the things that are making them different like Bloch functions, interactions etc. The next step would be to add interactions, mixing, splitting and then process to the other states as has been said at the beginning. This is a rather complex method, and the first thing you can do is to use the so called $k \cdot p$ perturbation theory to approximate some of the things and make calculations easier. As it is not the topic of the thesis, the places where you can read it further are here [46] [83] [25] [64]

2.4 PHOTOVOLTAIC DEVICES AND SOLAR CELL PARAMETERS

In this section we will provide the methods of solar cell characterisation and the quantities which are connected to it. More information can be read in [4]

2.4.1 PROPERTIES OF SUNLIGHT

The most important characteristics of the solar light are described by radiometric quantities. We will just state few of them. To finely describe the effects of sunlight we need to know:

- Spectrum of the incident light
- Radiation angle
- Radiant power density

PHOTON FLUX

Φ is simply stated as the number of photons per unit area in a fraction of time. We can then define the photon flux density to further divide it on the incident light wavelength. When we multiply ϕ_λ by the photon energy we get the energy per unit time, which is simply the power density.

$$\frac{\partial^2 P_\lambda}{\partial^2 x^2} = \phi_\lambda \frac{hc}{\lambda} \quad (2.4.1.1)$$

SPECTRAL IRRADIANCE

It is most common quantity to describe a light source. It is the power density for a certain photon frequency.

$$I_{e,\lambda} = \frac{\partial^2 P_\lambda}{\partial^2 x^2} = \phi_\lambda \cdot \frac{hc}{\lambda} \quad (2.4.1.2)$$

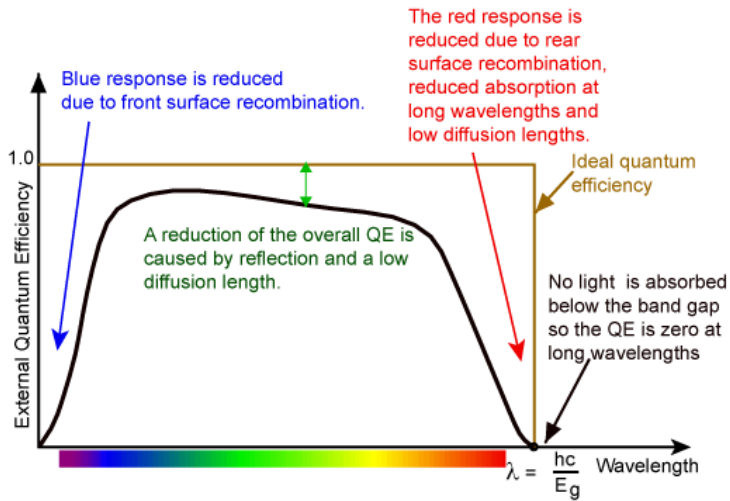


Figure 2.12: Quantum efficiency of an ideal silicon solar cell [4]

BLACKBODY RADIATION

Derived by Planck, this radiation law is described with spectral irradiance[66]:

$$I_\lambda = \frac{2\pi hc^2}{\lambda^5(e^{\frac{hc}{k\lambda T}} - 1)} \quad (2.4.1.3)$$

2.4.2 SOLAR CELL OPERATION

For a solar cell to generate current, the following main processes must be present. First one is the possibility to absorb photons from incident light so we can generate carriers. We must remember that minority carriers are only stable for a minority carrier lifetime before recombination. Therefore, before this time, we need to collect those carriers to spatially disallow carriers to recombine. Ideally, if we create pair in the n region, the electric field sweeps the minority carrier through the junction to the place where it becomes majority carrier. In a short circuit scenario, two carriers ideally meet together after flowing through the external circuit.

The fact that the carriers must "live" through the distance needed to separate them is described by collection probability, which depends on the diffusion length and surface properties.

The number of carriers collected in the solar cell compared to the number of incident photons describes the more macroscopic ability of the device. It is called a **quantum efficiency**

$$Q.E = \frac{\text{number of carriers collected}}{\text{number of incident photons}} \quad (2.4.2.1)$$

It is strictly dependent also on the absorption, so directly on the wavelength of incident photons.

It is also possible to describe an external QE(EQE), which also includes some optical effect such as reflection.

2.4.3 SOLAR CELL PARAMETERS

Here, we will state the most important parameters for solar cell characterisation, we will simply tell what do they stand for and how to measure them.

SHORT-CIRCUIT CURRENT

I_{sc} is the current that flows through the device providing that the voltage is zero across it (especially when we have short circuit). It comes directly from the generated carriers due to photogeneration and is connected to how well the structure can collect them or how strong the recombination processes are. It depends on:

- incident photons number (linear dependence on the incident power)
- solar cell area
- light spectrum
- optical losses (f.e. absorption, reflection etc.)
- real collection efficiency (its' probability)

We can clearly see, that this parameter allows us to differentiate between solar cells when comparing the ability to store generated carriers. (Remember, short-circuit current is not always the light generated current due to possible high series resistance).

OPEN-CIRCUIT VOLTAGE

V_{oc} is the voltage that is maximally available when using the solar cell. For that voltage, the current through the circuit needs to be zero. It states the forward bias that we need to put to compensate the light generated current. V_{oc} is logarithmically dependent on the incident photon power and it decreases linearly with temperature.

FILL FACTOR

When speaking about the above short-circuit current and open circuit voltage we are meaning the maximal current and voltage that we can achieve in the solar cell. Of course, as the momentary power is just their multiplication, therefore, at those times when we get each of the two listed quantities, the power is equal to zero. In order to still describe maximal power of the solar cell, people tend to use the **fill factor** FF.

$$FF = \frac{P_{max}}{V_{oc}I_{sc}} \quad (2.4.3.1)$$

where P_{max} is the maximal power achieved by the solar cell. It is the embodiment of the "squareness" of a solar cell. The higher the open circuit voltage, the bigger the FF.

PCE

From the FF we can derive another, probably most useful quantity, which has been yet used in the former chapters. This quantity is the **power conversion efficiency** PCE. It is a ratio of energy from the solar cell to the summary energy income from the Sun.

$$\eta = \frac{V_{oc} I_{sc} FF}{P_{in}} \quad (2.4.3.2)$$

where η is the PCE and P_{in} is the sunlight power.

2.4.4 SHOCKLEY-QUEISSER LIMIT

Also known as a detailed balance. It was a derivation of an idealistic maximum efficiency of a solar cell based on a p-n junction made by Shockley and Queisser in 1961[74]. The most common form of the implementation comes with fundamental assumptions:

- We have finite mobility, so the collection of the carriers can be performed anywhere.
- For wavelengths exceeding the band gap we have a complete absorption of photons.

In the principle, only photons with energy greater than the band gap can be absorbed and used in the generation of electron hole pairs. Generally, the electrons occupy the lowest level of the conduction band and so the exceed energy is released in heat in thermalisation process. For the idealistic model, they assumed that each photon with sufficient energy generates electronic charge q at voltage $V_g = h\nu_g/e$. E_g is the threshold for energy as the band gap, and as we stated before, we assume that all photons are absorbed above, so the function $a(E)$ (which used by the authors of the original derivation to restrain the integral only to the energies above E_g , just to fulfill the former assumption and is inserted there *ad hoc*) is equal to zero below E_g and unity otherwise. We can say that from the generated charge, the photocurrent density when shined with the photon flux Φ_{sun} is:

$$J_{sc} = q \int_0^{\infty} \Phi_{sun}(E) a(E) dE = q \int_{E_g}^{\infty} \Phi_{sun}(E) dE \quad (2.4.4.1)$$

Of course, to conceive the thermodynamic equilibrium, there needs to be an opposite process to absorption. We assume that the light emitted from the Sun is in the form of Blackbody radiation, as is the solar cell. The amount of radiation absorbed is the same as the emitted from the device to the environment with the same temperature. Therefore further it involves using a Planck Blackbody generalized formula for different energies above the band gap. Non-equilibrium radiation is only in a situation where the non-zero chemical potential of a radiation is present, and that is basically equal to a Quasi-Fermi level splitting(we have stated before that the splitting of a Fermi level is a non-equilibrium process). The photon flux emitted by a Blackbody with a bias voltage V is equal:

$$\phi(V, E) = \frac{2\pi E^2}{h^3 c^2} \frac{a(E)}{e^{((E-qV)/kT)-1}} \quad (2.4.4.2)$$

with c as the light vacuum velocity, k as a Boltzman constant, T as a temperature. This emission is connected with a recombination current density $J_r = q\Phi_e$, where Φ_e is an integration of the flux density over all energies. In thermal equilibrium both currents are equal. When we apply voltage, we know that the current is a Shockley equation (Eq. 2.2.7.5. Maximal voltage is ideally the $V_{oc} = kT/q\ln(J_{sc}/J_0 + 1)$, yes, it is the open-circuit

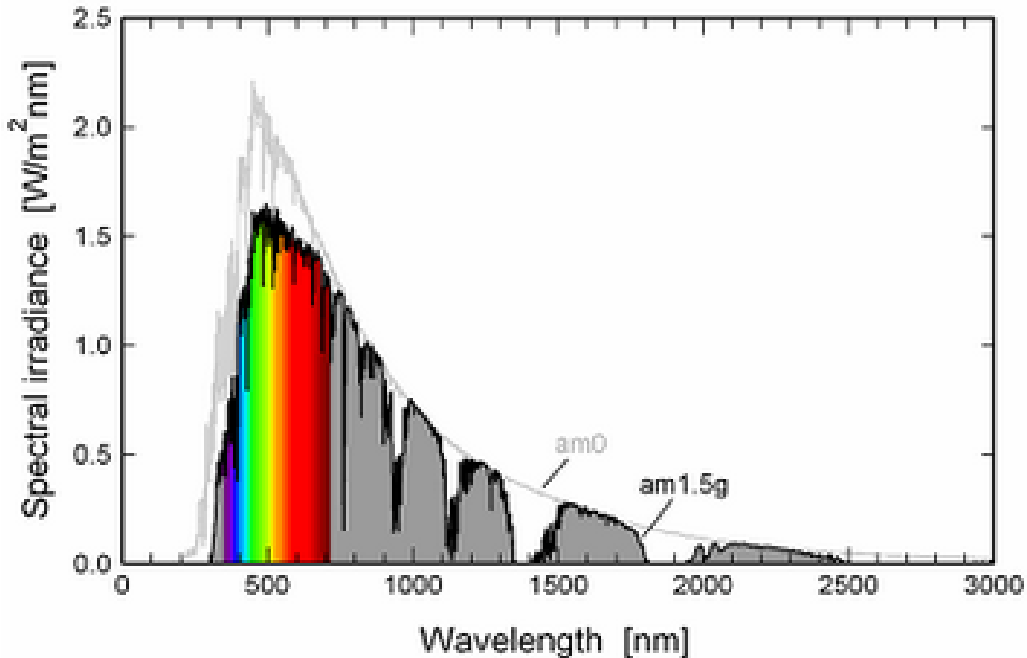


Figure 2.13: AM1.5 irradiation at Earth surface[5] and AM0 at Earth's orbit

voltage and $J_0 = q \int a(E) \phi_{abs}(E) dE$. Now, connecting this with AM1.5G spectrum, which is a standard spectrum for using solar cells, we can get that normally, for solar cells with band gap within 1eV to 1.5eV, we can get the maximal efficiency of 33% . [74]
In exceeding the SQ limit we can use for example:

- Tandems
- Magneto-optic devices
- Hot carriers(strong electric field effects)
- Multiple exciton generation(as in Quantum Dot Solar Cells it is possible to create more than one exciton from one photon!)

2.4.5 EFFECTIVE RESISTANCE

To include some of the resistive effect on the solar cell and still use a model similar to the idealistic one, one uses series resistance and shunt resistance. Their main impact is on the FF of the device. Their dependence is on the geometrical properties of the solar cell. The series resistance has it's origin at three physical places: the emitter-base current, contact metal-semiconductor and top/rare contacts resistances. To include it we simply write the current equation as.

$$I = I_{lg} - I_0 e^{\frac{q(V+IR_s)}{nkT}} \quad (2.4.5.1)$$

where n is an ideality factor and R_s is the series resistance. The rest is taken from Eq.(2.2.7.5).

For the shunt resistance the case is about the defects from the manufacturing. It simply takes away the factor $\frac{V+IR_s}{R_{sh}}$, where R_{sh} is the shunt resistance. [4]

2.5 QUANTUM DOTS AND QDSSC

2.5.1 SEMICONDUCTING QUANTUM DOTS

Due to their practical application and rather easy, yet not really repeatable fabrication, semiconductor quantum dots have made a vast impact in all technology. Their potential confinement in all three directions allows to profit from many new possibilities, not known in solid state physics before. We can easily distinguish three different categories for their production which are:

- Self assembled QDs
- Colloidal QDs
- Electrostatically defined QDs

Considering the fact that we are only using the second ones, we will mainly focus on them.

COLLOIDAL QUANTUM DOTS

To put it straightforward, CQDs are semiconductor crystal of nanometre scale size, with diameter less than twice the Bohr radius, which are synthesized(deployed) by nucleation in colloidal solutions. They are surrounded and restricted by surfactant molecules called ligands.

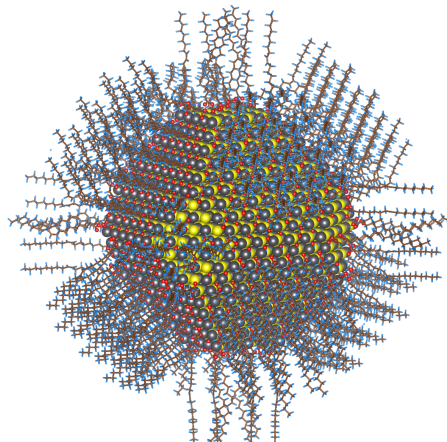


Figure 2.14: Image of ideal CQD composed of selenide with passivation with oleic acid, oleyl amine and hydroxyl ligands [6]

They have manifested to provide a development of numerous types of optoelectronic devices including photo-diodes and PV devices. The properties of CQDs are easily adjusted by changing the volumetric features of nanoparticles similarly to metallic nanoparticles in plasmonic transport. [9] [26]

Even though we don't focus on the synthesis of particular used CQDs, it is instructional and scientifically appropriate to be slightly familiar with it. It consists of three-component solutions, which are precursors, organic surfactants and solvents. In order for get the precursors transformed into single chains called monomers, the probe is heated to high temperature(they have enough energy to get separated), then, when there's enough of them, the monomers are growing into crystals. Of course, the temperature shall be manipulated

with a dose of care because when it's too high the crystals aren't forming fine or at all. When we achieve optimal saturation of monomers, we get quite even growth of all particles, (small ones grow faster than the heavy ones) and it has to be sustained in order for the homogeneity to be achieved. Typically, CQDs create alloys, binary or ternary, and contain 100 to 10^5 atoms. Usually, they confine all carriers inside the volume.

QUANTUM DOT SIZE

With changing the size of the nanoparticle we can control the band gap over significant range of spectrum. Yet, practically, the width of the nanoparticle is estimated from the energy band gap. [92]

QUANTUM DOT SHAPE

The geometry in physics plays an important role, there is no question about that. It is obviously not different for Quantum Dots. The quantum confinement strongly depends on the shape and dimensional geometry. The ability to control the growth of certain form allows the nanoparticles to exhibit a variety of properties.

2.5.2 CORE-SHELL CQDS

Modification of the standard synthesis methods allows us to create new behaviour and improvements in nano-structures characteristics. For example, in this method, same type, but different semiconducting nano-crystals are grown around the first ones(core). They tend to achieve better luminescence than the former because we simply drastically cut the possibility of non-radiative recombinations between energy levels. We can differ type 1 structures using conduction band of the core below the shell energy level(the core confines all carriers inside because of the energy minimisation) and in the second type, the energy levels are mixed so only one type of carriers is confined to the shell and the core. [67]

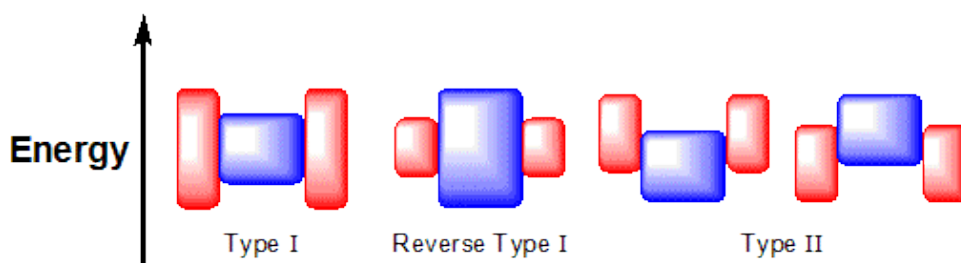


Figure 2.15: Types of Core-Shell CQDs(blue color is core energy structure), we can see that in the first type both electrons(smallest energy in CB) and holes(biggest energy in VB) are confined beneath the core. [7]

2.5.3 CQD SUPER-CRYSTAL

With CQDs we can even create super-lattices(layers of few materials which create a periodic structure). In order to achieve the fine quality of them we need to have an absolutely outstanding transport properties. [31]

FURTHER READING FOR CQDS

More about synthesis and theory of nano-crystals and thermodynamics can be read in [46], [21]

2.5.4 PRINCIPLES OF QDSCS

Quite early, because in fair 1960s, the idea of harvesting sunlight with using sensitized semiconductor devices with generation of carriers inside narrow band semiconductors has been proposed. The usage of colloidal quantum dots has produced new possibilities and shown amusing prospects for using nanotechnology. The properties can be tuned by changing the QDs size itself which means changing the size of electronic band (relocate CB - conduction band and VB - valence band) depending mainly on effective masses of the carriers. The electronic shift that we can achieve by relatively simple parameters manipulation will provide a shift of VB edge downwards and CB upwards, as a result of a, quite important in this scale, quantization of energies. As we know, besides band gap enlarging, it also changes the driving force for carries injection and this is most important part, as we want to use them as an amplifier in the PV devices. The great achievement of these types of solar cells is the decoupling the charge generation and its transport to different materials- the hole and electron transport layers. The effect of such a procedure is the decrease in recombination process and reduction of production costs. Without that technique, the architecture is adequate to the standard PV solar cell device. The generation of electron-hole pairs proceeds the injection of electrons from CB of light harvesting material to electron acceptor layer and holes from VB to hole acceptor layer. We call this process a charge separation. Nevertheless, even though we do regenerate QDs in the light harvesting area after charge separation, we still have to struggle with recombination processes and consider them as the significant performance wasters. [71] There are few commonly used configurations of solar cells based on those previously mentioned nano-crystals and are shown in 2.16

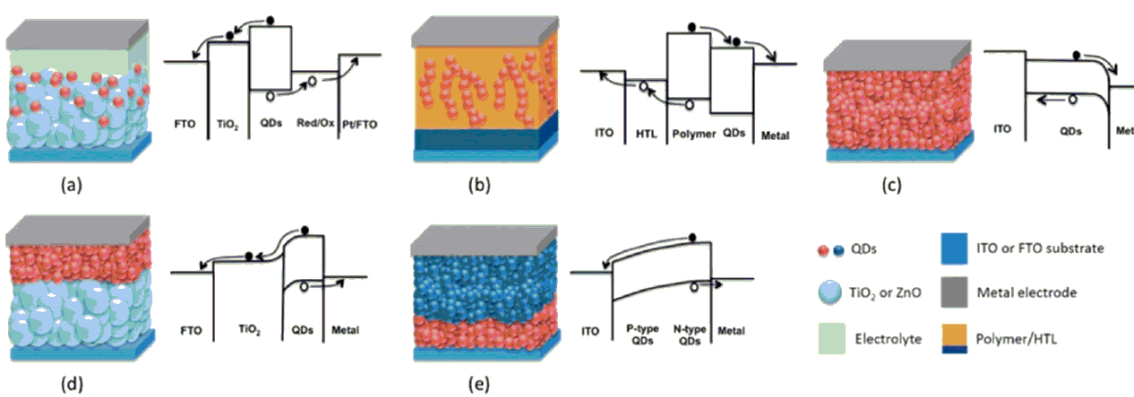


Figure 2.16: Schematic illustration of configurations and band structures of QD solar cells:
a) QD-sensitized b) hybrid QD-polymer c) Schottky junction d) p-n hetero-junction e) p-n homo-junction [35]

Schottky schematic is a type of device where thin QDs film is placed between two contacts and is used for generating electrons and holes. The barrier, which is created between the low-work metal and QDs layer, is quite similar to bulk one where the potential is bent

proportionally because of the charge transfer between the layers that touch. From them, few very unique and promising short currents have been achieved. Unfortunately, low open circuit voltages are present for them because of the pinning of Fermi level. Then, we have the depleted heterojunction, where we use wide band gap oxides such as ZnO on a conducting glass. After that we put some QDs films above that and end it with a fine metal contact. The oxide layer behaves as layer for electron conducting phase, so the metal contact extracts majority carriers. There we have more of a compromise between I_{sc} and V_{oc} . The next type is a hybrid QD-polymer solar cell, where electron is transported and photon absorbed both in the QDs layer (with the polymer film together). The PCEs of such attitudes to the device engineering is still smaller than the former ones, probably due to not optimal hole transporting layers. P-n hetero- or homo- junctions are both traditional methods of harvesting and transporting the light but instead of using bulk semiconductors, we use semiconducting QDs.

The Quantum Dots Sensitized Solar Cells (QDSCs) are devices in which QDs are not the most important part when considering the carrier transport. The idea was to replace dyes with QDs, but the rest of components has been still based on the concepts formed by their ancestor. Sadly, not too late after, it was realised that it's not so similar at all and some of the components need to be redesigned from scratch. However, even though the DSCs are easier to achieve the better performance with, the QDSCs are more promising and theoretically can be cheaper and have longer lifetime. Inside the device structure, the QDs itself are responsible for light absorbing and carriers creation. Then they are divided in different layers so obviously the great PCE can only be achieved if large incident photon to current efficiencies (IPCE), V_{oc} and fill factor are possible.

$$IPCE(\lambda) = LHE(\lambda)\phi_{inj}\eta_{col} \quad (2.5.4.1)$$

Where η_{col} is electron collection efficiency, ϕ_{inj} is electron injection efficiency and of course $LHE(\lambda)$ is left to be the light harvesting efficiency, so it's directly connected to absorption and automatically to QD loading and the band gap, as has been seen in theory chapter. The loading only depends on the quantitative parameters of transport oxide layers such as thickness, particle size and coverage degree. The injection then depends on how fine would we attach both layers together and the collection efficiency will consider the interfaces and the internal structure of transporting phases. Of course this means, as in all of the solar cells, high mobility with relatively slow recombinations in the main energy regime. We can now clearly see that the big advantage of those cells is that they separate the ideas of charge generation and transport to different parts, so it gives more possibilities to engineer new materials. [35] [84]

2.5.5 MATERIALS AND PERFORMANCE DEVELOPMENT OF QDSSC - A REVIEW

1. Electron Transporting Materials (ETM)

They are used to support charge separation as briefly described above. The function proceeds as a support for QD in the charge generation layer, as it transports charged electrons to the conductive substrate (usually ITO or FTO). [85] [79] The properties shall be as follows:

- Matching CB edge which will determine exciton generation and partial transfer efficiency.

- High electron mobility.
- Fine surface to provide suitable loading of particles.
- Suitable technological properties, such as stability, low cost etc.

The most widely studied materials nowadays are TiO₂ and ZnO. Materials based on the first one are of such importance due to their non-toxicity, chemical stability and low cost [36] [79]. Among them (TiO₂-NP) based mesoporous layers are researched as photo-anodes [36]. The highest efficiency ever recorded(up to 2018) were based on that material [20] [40]. Unfortunately, the probability for charge recombination in that kind of films is rather unsatisfactory. Therefore, one provides one-dimensional structures such as nano-rods and nano-wires to maintain fairly smoother electron transport channel and decrease loses provided with recombination [87] [52]. In 2007 it was shown that TiO₂ nano-tubes win over nano-particles of the same material in case of transport capacity [44] [80]. Thus, the research of such structures was accelerated and many brand new CdSe sensitisation methods were proposed [89]. After that, many different sensitisations were provided, in which also PbS QDs had their small part [14]. Although promising, the 1D structured TiO₂ based anodes were unsatisfactory in case of PCEs, when comparing to standard nanoparticles (maximum of around 6%). The hypothesis was put on insufficient loading amount on 1D structured TiO₂, therefore the focus should be put on improvement of that area. A group of researchers has also used graphene frameworks incorporated into TiO₂ photo-anode achieving 4.2% PCE for QDSSCs. [86] By using double-layered films with particles of bigger volume, there has been achieved a high PCE of 4.92%. A lot of dopants and different solutions, hybrid photo-anode films with metal and non-metal ions and carbonaceous layers has been proposed to improve performance of PV devices. Also with the usage of hollow structure techniques, by creating nano-tube arrays, the possibility of achieving a PCE of 6 % has been shown [56]. Improvement in light absorbance was achieved by using microporous TiO₂ photo-anode for PbS quantum dot sensitised solar cells achieving up to 3.5% PCE performance.

In case of ZnO based photo-anodes the differencing property is a higher electron mobility and better conduction band edge. With them, the achievement of higher V_{oc} is more probable [85]. Unfortunately, the chemical stability of those films is significantly lower. Similarly to the former, the nanoparticles were widely studied. [48] As an example, the CdS sensitised ZnO nanoparticles were used to construct a photo-anode, which allowed the achievement of 4.46% PCE. They used TiO₂ passivation of ZnO surface to improve the PCE of same sensitized CdS/ZnO QDSCs by more than 2%, achieving 4.68% [97]. Similarly, the 1D structures for ZnO can be crystallised. The distinction from the former is the ease of it's development. The ZnO nano-wires sensitised with CdSe constructed in 2007 were the launch of the technology development and allowed Young et al. achieve PCE of 4.15% [41]. Many more one dimensional structures of ZnO based photo-anodes were used to research maximal performance but it was shown that the problem again concerns the surface area [29]. The second strategy to improve the performance of such material based structures is double layer replacement with two different 1D structures such as NR on bottom and TP on top. However, the PCEs of ZnO based films still stay behind TiO₂ ones.[97] The Al/Cl hybrid doping allowed to use ZnO in IR spectrum.

There are other kinds of ETMs researched as well. Using big tandem structures has manifested superb PCE through simulations [30]. The doping of synergistic

fullerene electron transport layer has proven to increase solar cell performance [62] . A series of materials such as SnO₂, NiO, BiVO₄, Zn₂SnO₄, BaTiO₃, CoO have been incorporated to QDSC manifesting future potential. High performance has been achieved using CdS thin films as single-source precursors to ETM layer providing over 8% PCE. [70]

All of the above materials are n-type semiconductors. Furthermore shall we proceed to introduce the p-type metal oxides and p-type Quantum dot sensitised cells. Typically, the NiO semiconductor is widely used. The promising and comprehensive material that can be implemented is CuSCN, which is an inorganic of p-type. Of course, the extraction of a hole from light harvesting layer to a redox couple will be rather slower than in case of electron. Therefore, being the potential solution to this problem, the p-type semiconductor based layers are beginning to leave their mark in PV devices. As expected, the most accurate application of that type of films would be the tandem configuration construction, which contains both n-type and p-type QDSCs to overcome so called a Shockley-Queisser limit. However appealing, the efficiencies of p-type QDSSCs are yet to be enhanced.

2. Hole transporting material (HTM) layers

The electrolyte or HTM is crucial to QDSSCs as well. The properties of such film shall be:

- Low corrosivity.
- Red-ox potential appropriate to regenerate QDs and maintain fine V_{oc} .
- High conductivity through ions.
- Stability and transparency in visible spectrum.
- Possibility to fully regenerate. [35]

The common electrolytes:

- **Liquid electrolytes**
- **Quasi-solid state electrolytes**
- **All-solid state electrolytes**

were described comprehensively in the following research papers [35] [95] [76]

Although using Sb₂Se₃ as a thin light harvesting film, a group of researchers has also used PbS colloidal quantum dots as a hole transport layer achieving 6.5% PCE in 2017 [82]. Earlier, the usage of graphdiyne(a novel large π -conjugated carbon hole transporting material) has allowed an efficient hole transport layer for solar cells based on PbS-EDT colloidal quantum dots[57]. Before that, in 2015, colloidal CuInS₂ QDs were layered to hole transporting solution and, even though the scientist did their research on Perovskite solar cell, they accomplished to get almost 8.5% PCE[43]. The extended device stability and a rise to 10.6% of PCE was certified using CQD solar cells using P3HT as a hole transport material [96].

3. QD sensitizers

The main part of our PV device, the QDSC are QDs. The ability of harvesting interfering light is a crucial component of such device. [37] Therefore, the ideal nano structures should exhibit certain properties:

- A higher conduction band edge than the one in the electron transport material and lower than in hole transport material to provide effective charge separation.
- Obviously, as in all semiconductor PV devices, we shall provide a material with accurate band gap, ideal for our purpose. The reason is clear, we are interested in superb absorption in wide range of solar spectrum.
- The stability is the crucial property as well.
- From the technological point of view - the simple preparation and of course low toxicity would be rather expected.

Therefore, we will now examine methods to deposit them and the differences between certain QDs materials.

Deploying on the surface

Because of QDs being inorganic and possessing larger size than simple molecular dyes, they are much more difficult to tether onto metal oxide to form a high quality mono layer. Therefore high QD-loading amount is rather high to achieve. We can difference the deposition methods by putting them into two categories: *in situ* and *ex situ*. In the first one, the QDs are grown directly on the surface of the metal oxide substrate, being created using an ionic precursor. We can include chemical bath deposition(CBD) and successive ionic layer adsorption and reaction(SILAR) into this category. The second approach bases on pre synthesising of QDs and then depositing them onto the metal oxide. Easily processable and finely reproducible, the *in situ* method has been used more widely than its' counter. In that kind of deposition we can control not only the QD-loading amount but also size distribution. Unfortunately, the achieved density of trap states is rather high, therefore the obtained maximal PCE is about 7% [49]. In this case, excluding the QDs growth process, we have to accurately deploy them onto the surface. The most common methods are: direct absorption, linker-molecule-assisted self-assembly, electrophoretic deposition. [35]

Ligands

The ligand part in QDs is, as mentioned before, the important part of obtaining high efficiency of QDSCs [72]. The comparison of halide ligands in PbS CQDs for field effect transistors(FETs) has been made by researchers in 2018[11]. The capping-ligand-induced self-assembly method was the clue for TiO₂ photo-anodes[35]. Nevertheless, researchers haven't discovered a satisfying approach yet. In 2012, the deposition method were optimised through using ligand-exchange techniques.[16] Thanks to that, the PCE record of 13% was achieved [81]. Not only CLIS deposition has been used. The aqueous solution provided the simplification of QDs fabrication with shorter ligands. Some relatively high PCEs have been achieved with that method. Then, the organic molecules usage allowed scientist in 2015 to achieve 3 times bigger PCE compared to common creation of PbS quantum dots.[38] The certified PCE of 11.21% has been achieved via so called "solvent curving", which is the simplified

method of PbS QDs fabrication processing. The passivation of PbS QD surface with L-glutathione was used to produce QDSSCs with promising results.[19] 10.6% PCE was achieved thanks to solvent-polarity-engineered halide passivation [61].

Binary structures

Up to date, binary QDs have also been used as sensitizers. There are many examples but the most common are: InP, InAs, CdS, CdSe, CdTe, Ag₂S and with them, the most interesting one considered in our case - PbS.[63] [88] The main problem with them is to control and balance the narrower band gap and relatively high conduction band edge. For example, for PbS nano crystals the band gap is narrow, but the conduction band edge is rather low, which causes the problem and has to be dealt with. In case of binary QDs we have to balance between the light harvesting efficiency and efficiency of charge injection. Mixing binary structures (for example PbS with PbSe) has been also proven to enhance the interesting efficiency[75] [24]. Treatment of PbS QDs with metal salts provided some advantages in CQD PV devices resulting in the increase of short circuit current and fill-factor [54]. The crucial part of success in getting high efficiency would also be suitable engineering of solvent[93].

Core shell QDs usage

The other methods to use QDs as sensitizers in PV devices is creating a Core/Shell QDs. Their unique properties have been mentioned before. The alignment in these provides ability to tune the light-absorption range, recombination processes and charge separation. Usage of them in QDSCs is rather modern. The first noticed implementation was created by Lee et al. in 2009. Through SILAR method, he achieved PCE of 4.22% [50]. Yet the difficulties in creating specific materials may occur, because of inability to prepare a stable precursor for deposition methods.

Alloyed QDs usage

The massive perspective in PV devices has also been established by using Alloyed QDs. These allow us to create the non-linear band gap [68]. Stability in such materials is again much higher than in their constituents. A lot of scientific research was done in that area.

Doping

We can also include dopants to QDs. There were a handful of propositions in the [35] review. Yet, the promising idea has been introduced with the usage of metallic nanoparticles dopants by considering plasmonic physical phenomena.[47] [91]

4. Counter electrode

As we may already expected, they are also playing an important role in achieving high performance of PV device. The electrodes have to catalyse reduction reaction. These shall poses properties as follows:

- Good conductivity
- High catalytic activity
- Fine stability, either chemical and physical

We can also put them into four categories:

- **Noble metals**
- **Metal chalcogenides**
- **Carbon materials**
- **Composite CEs**

Recent progress has been comprehensively described in those publications. [90] [35] .

CHAPTER 3

PREPARATION, DEPOSITION AND OTHER EXPERIMENTAL METHODS

3.1 QUANTUM DOTS PURIFICATION

After the synthesis, the lasting of many redundant impurities inside the solution provides unwanted complications such as lower photo-luminescence, faster oxidation or potential problems with the traps. Therefore, separating our beloved nano-crystals would be crucial for achieving the purity of the device. The impurities that did not react during the process are a large scale particles that can be filtered by many different methods. [73][51] To do that, people usually change three main properties of the QDs solution which are: polarity, size and mobility. For any colloidal system, the challenge that we approach is not only connected with the type and the amount of ligands connected to the core crystal but the solvent properties as well so the parameters may change in a real time for any of the part and we need to be really careful not to change any drastically.

3.1.1 PURIFICATION METHOD

For our case of PbS nano-crystals, the method used was a polarity based purification technique. There are two most common processes in which we can clear the untidy system when considering only polarity. It is either precipitation and re-dissolution (PR) method or extraction method.

The first one is frequently used in case of non-polar solvents and thanks to the anti-solvents introduction the polarity of the solution is increased. Then, the retaliation of the impurities via the supernatant(which is the mixture that is floating after the centrifugation of the suspension) is taken away and we are left with quite pure nano-crystals which can be the redissolved in clean solvents. The repetition of the process is available for us for several times but not infinitely, because we can misleadingly get rid of ligands, which are necessary in chemical non-static processes that occur inside the solvent. It has also been seen for many times, that larger particles are more able to participate in the polarity induced precipitation than the smaller ones which means it's harder to get rid of the later ones. The method isn't always accurate because of the ability of the ligands to dissolve which can be really similar to the nano-crystals. More can be read in publications mentioned in the beginning of the chapter. |

3.1.2 METHOD'S PROPERTIES

POLAR/NON-POLAR PURIFICATION METHOD

The first thing to do was to add chloroform to the nano-particles dissolved in CHX(cyklohexane) solution. CHX is the standard cykloalkane used in case of quantum dot nano-crystals. The amount of the liquid was about the former amount of CQDs solution. Then, to begin it's work as a purification mixture, we added polar solvent acetonitrile. The unwanted particles and some of the wrenched ligands are then separated using the centrifuge. Carefully, in the nitrogen created vacuum, we separated the supernatant because of the danger of PbS fast oxidation. Chloroform was then again used as a solvent for now clean CQDs.

3.2 DEPOSITIONS PARAMETERS AND METHODS

After successfully purifying the Quantum dots, the time for the deposition has come. We will now discuss used methods and then show the schematic for the steps taken in creating the device.

3.2.1 GLASS CONTACT CLEANING

To be sure that we can reduce a number of defects connected with dust and air pollution, the transparent glass contact needs to be cleaned. It is done with simple method using a strong detergent and solvent(in our case isopropanol). The glass is placed inside the holder and put in deionised water for rinsing. After few times, when the glass is clean it is then placed in the UV-ozone cleaning chamber. Inside, UV lamp either dissociates Oxygen into triplet and then it combines with O_2 generating ozone or with the higher wavelength dissociates O_3 and makes singlet oxygen in the process(it reacts with substrate surfaces strongly). It is a dry process, in which there is a low damage on the probes.

3.2.2 SPIN COATING

To achieve an uniform deposition, the technique of applying a small amount of rotating material is used. The centrifugal force achieved with rotation allows to place the substrate only if it's possible to convey it on the surface for a longer period. Usually, as also in our case, the substrate can simultaneously evaporate during the process. With the angular speed, the thickness of a layer is parametrized, so higher the velocity, the thinner the layer.



(a) Ionized water cleaning equipment



(b) UV-ozone cleaning equipment

Figure 3.1: Cleaning methods environment



(a) Glovebox used in the laboratory



(b) Spincoater used in the laboratory

Figure 3.2: Laboratory equipment view

3.2.3 GLOVEBOX

It has to be highlighted that some of the processes cannot be done with the contact of air. Therefore, a single machine called glovebox is used to overcome some of the task and to ensure even higher quality of the out-coming creation. Inside it, the inert atmosphere is made with using nitrogen so the items need to be inserted with vacuum pump.



Figure 3.4: Sputtering deposition device that we were using

3.2.4 SPUTTER DEPOSITION

After creating the distinct and separate layers for transporting and absorbing parameters we have to create a second contact for the device. In our case, the sputtering method PVD is used. It uses a material called a target(an item consisting of a desirable material) from which parts are ejected into the substrate. The sputter gas is pumped into the chamber, where a magnetic and electric fields are both confined. The gas atoms thump target ions which create the plasma in the chamber and then they hit the substrate.

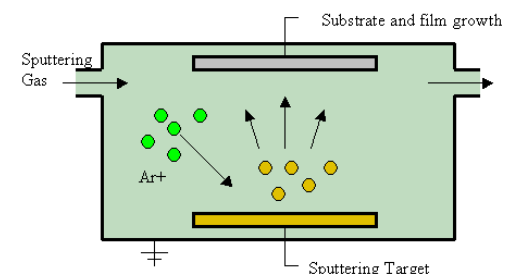


Figure 3.3: Sputtering deposition schematics(https://www.wikiwand.com/en/Sputter_deposition)

CHAPTER 4

RESULTS AND CONCLUSION

4.1 PbS QUANTUM DOT SOLAR CELLS

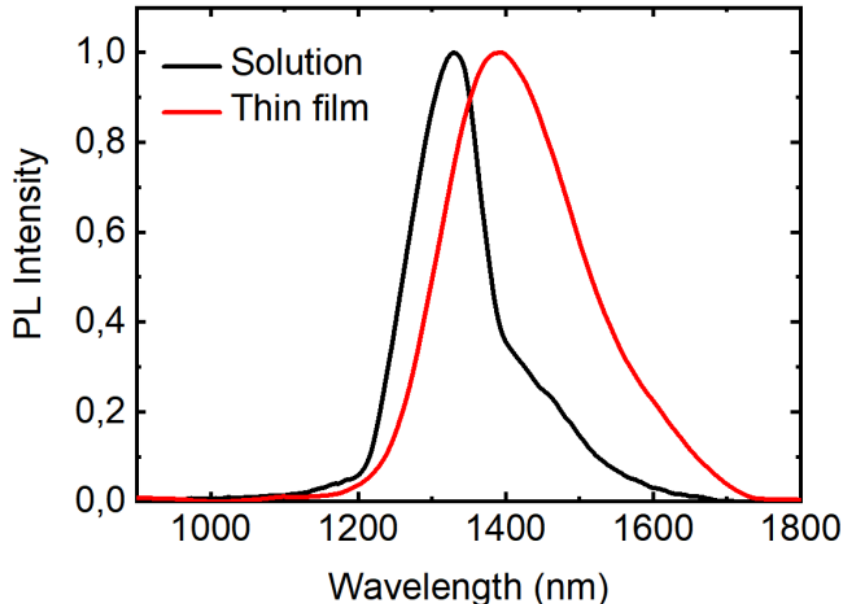


Figure 4.1: Emission spectrum of used PbS QDs [1]

The whole idea of all-solution processed QD solar cells is beginning to mark its footprint in modern photovoltaics. Within all of type III SC PbS QDs are promising candidates and certainly a field of quick improvement. Yet, what is so promising about them and what are the features that distinguish them from other types. In case of PbS QDs it must be denoted that the main advantages that they provide are the high efficiency and wide bandgap tunability due to its direct link with quantum dot size. For photovoltaic purposes the next important thing would be the ability to multiple excitation through the band gap.

They are used in many different structured solar cells, creating a numerous variations of junctions and quantum dot treatments and achieved over 11% power PCE as for last few years. The main problems with them would be to conduct and choose a fine ligand passivation. In our case the halide anions from precursors of tetrabutylammonium iodide (TBAI) and 1,2-ethanedithiol (EDT) were used. Ligands from such precursors do not only,

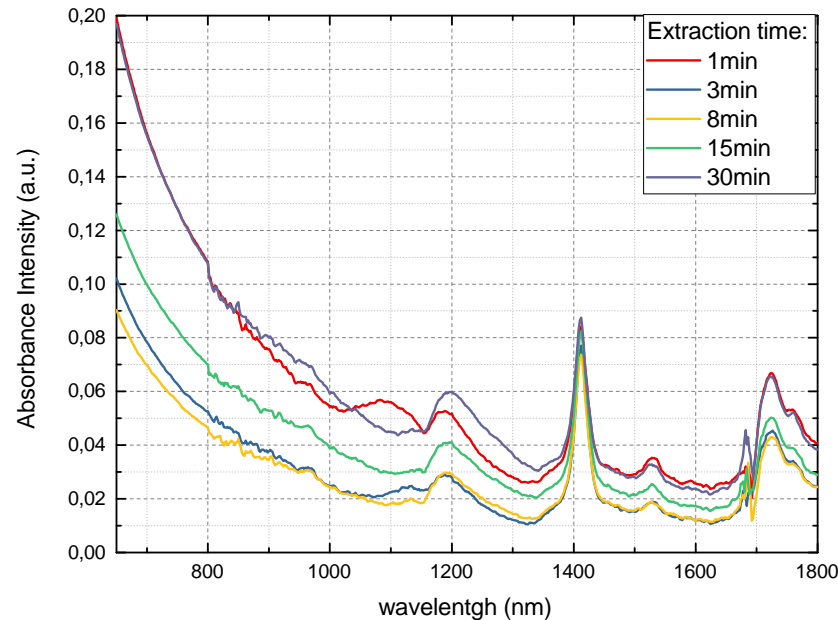
more or less precisely, passivate surface defects, which are of course unsatisfactory for our case, but modify electronic properties of QDs as well. The PbS-EDT layer was used as hole transport and PbS-TBAI, a main light harvesting layer, has been reported to usually be a n-type semiconductor, probably owing to a) I^- anions that are exchanged in PbS QDS with S_2^- and b) I^- anions are bound to the surface and repulse oxidative processes. We have chosen both types of ligand passivation as it has been proven that solar cells that use layers of both materials have manifested the improvement in air-exposure stability when compared to the devices that use only PbS-TBAI [27]. Although a longer air-exposure provides undesirable consequences that downgrade the cell significantly, the short period exposure is suspected of creating a more efficient charge extraction. Nevertheless, the inner processes that allow that bi-layer structure to be one of the best, provided for those types of QDSCs, is still vague and further improvements are expected if it becomes much more understood. For example, a greatly simplified deposition has been achieved by replacing methanol with acetonitrile, which consequently improved electrical properties of photovoltaic device as well[12]. (The device structure was very similar to ours). There are irrefutable results in achieving fine results from synthetisation from the group[82] [34].

4.1.1 PbS QUANTUM DOTS PRODUCED IN OUR LABORATORY

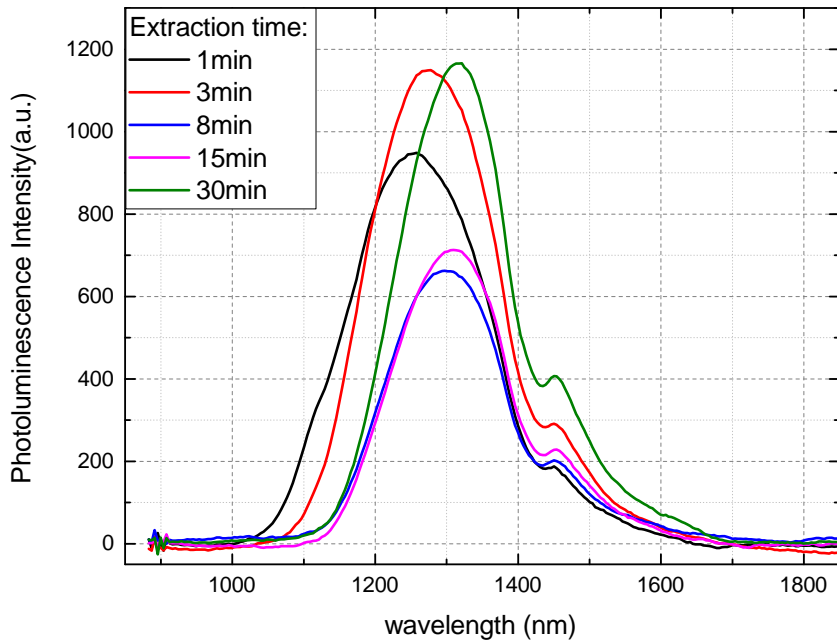
The manufacture of CQDs is an effect of cooperation between the group members, and the results in the synthesis of PbS Quantum Dots are ought to them. Those nanostructures are similar from time to time, yet being improved with each synthesis. We will discuss the effects shortly but more can be found in [77], which is a complementary thesis to this one, done by a student from the group. Fig. (4.2b) shows us the different optical measurements of the synthesised QDs. The synthesis has been made in 80deg C, which means that the sulfur solution was injected at that temperature. The synthesis method is described in [77] and is based on [53]. The labels on the graphs show the time after which 0, 1 – 0, 15mL of solution was extracted. Then, for measurements, the solution was dissolved in chloroform(CFL), for which the ratio was 50 μ L/2mL. Both spectra exhibit the difference as the QDs grow during the processes before they were extracted. To be noted, we can also see the solvent resonances present in both spectra. Mind that the width in luminescence spectrum isn't yet sufficient, as we would like to reabsorb only small amount of the photons to reduce phononic effects. Also, the absorption spectrum is really impressive with few peaks overlapping with solar spectra, as we would like to extract electrons where the intensity is the highest. Fig.(4.2b)

4.1.2 FIRST DEVICE DEPOSITION

A first insight of what can we do and what would be the challenges to overcome has been made due to creation of a first working solar cell. Fig.(4.4) shows the first device which will now be introduced below. The cell was based on PbS QDs and it has shown a promising quantities for further development. The whole subchapter provides a comparison of Vimun SC-3514 3rd generation silicon solar cell and our own QDSC.



(a) Absorbtion spectrum



(b) Photoluminescence spectrum

Figure 4.2: Optical measurements of QDs synthesized by [77] and the procedure is described right there. It is worth to mention that the injection has been made at 80deg C. Graphs were included with kind acceptance of the former thesis author



Figure 4.4: First device and PbS Quantum-Dots produced in our laboratory

DEVICE FABRICATION

The support for a whole device was ITO-coated glass substrate that was cleaned with strong solvents and drained ultrasonically. After that a double layer of ZnO was created by using a spin-coater and after annealing PbS QDs were fabricated using spin-coating as well. It is important to denote, that it was possible to create a multi-deposition layers of QDs, which means the structure isn't eluted from the ground. The layers were successfully dried in vacuum. After that, a MoO_x firm has been added for creating inside trapping states and with sputtering process Al contacts were created on the device. As many heavy-metal QD semiconductors are toxic and degrade in air they must be also encapsulated in a stable polymer shell to avoid exposure.

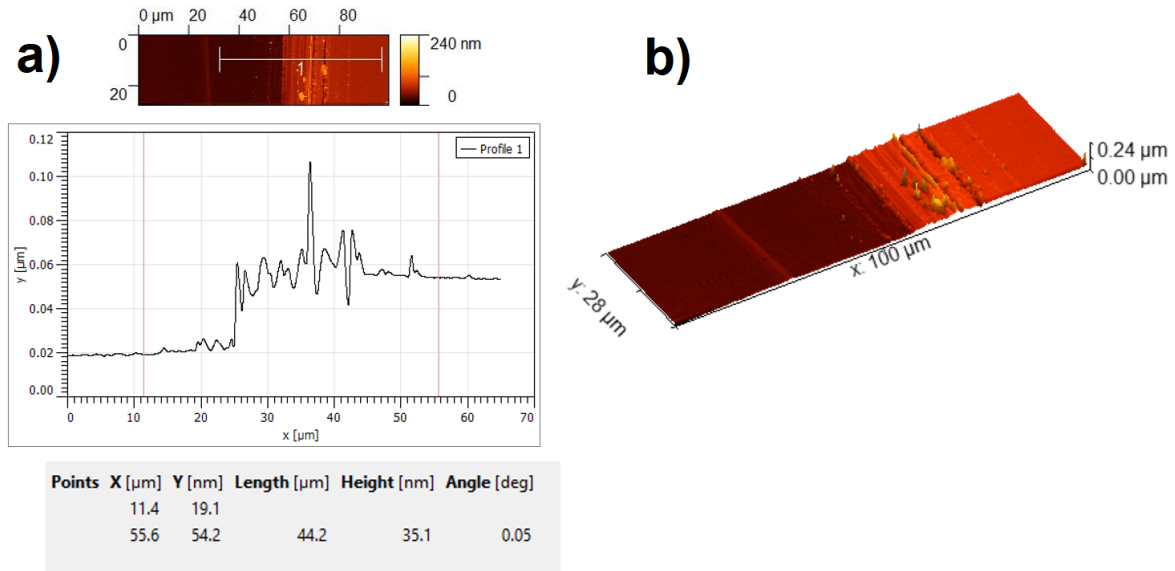


Figure 4.3: AFM picture of deposited ZnMgO layer b) and it's cross section a)

Fig.(4.3) shows the ZnMgO layer deposited on the ITO glass contact. On the a) part there is a cross-section visible. From that we can clearly see the border between two materials. The width of the layer is estimated to be $0.04\mu m$ taking the average line.

RESULTS

From the calculations below we will be able to compare both of the solar cells to distinguish what shall be improved to achieve better effects. Standard photovoltaic measurements were done to describe both devices. However, it has to be denoted that for the bright IV characteristics neither were the surfaces of both devices the same, nor were the lengths from the light source and it had to be included in the later reasoning. Therefore, a certain calculations and assumptions were made.

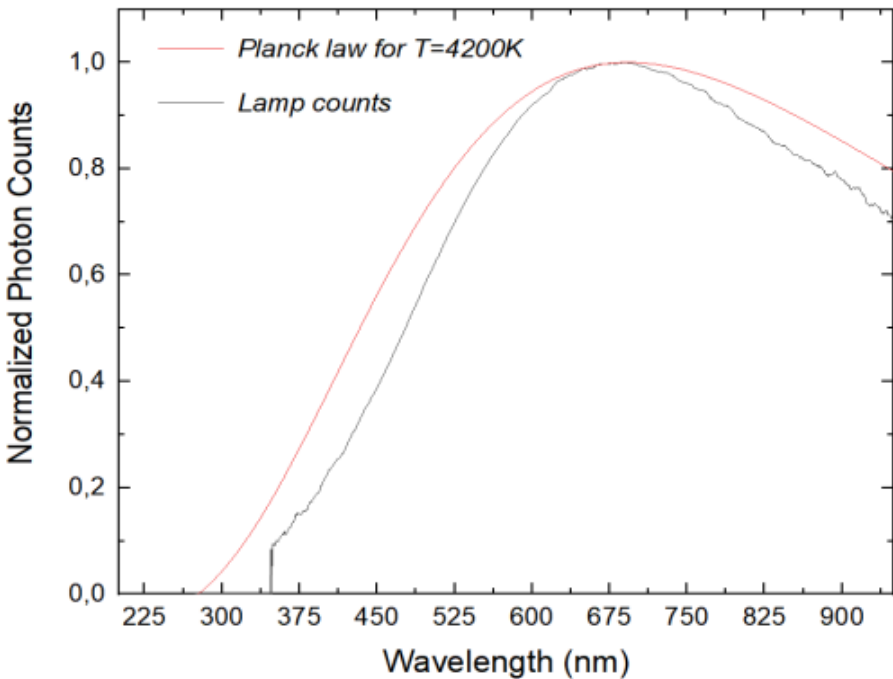


Figure 4.5: Comparison of Black Body photon counts and that of our light source

From the photo-diode detector which were illuminated from the light source at $h_d = 400\text{mm}$ we calculate the P_d - power on the detector. We know that the photo-diode responsivity:

$$R_\lambda = \frac{I_p}{P} = \frac{I_p}{r_p \cdot \frac{hc}{\lambda}} \quad (4.1.2.1)$$

where I_p is a photo-current output, and P is a ratio of radiant energy incident on the photodiode, which directly enables to calculate r_p – photon flux(number of photons/sec). We also define quantum efficiency of a photodetector as:

$$\eta = \frac{r_e}{r_p} \quad (4.1.2.2)$$

which is the number of light created electrons to number of incident photons. That depends on wavelength through absorption coefficient, thickness of layers etc. Therefore we can say that:

$$r_e = \eta r_p = \frac{\eta P}{\frac{hc}{\lambda}} \rightarrow I_p = \frac{e\eta P}{\frac{hc}{\lambda}} \quad (4.1.2.3)$$

Now, responsivity may be written as:

$$R_\lambda = \frac{e\eta P}{hc} \quad (4.1.2.4)$$

According to those calculations we now see that from:

$$J_{sc} = e \int_{\lambda} \Phi_p(\lambda) \cdot \eta(\lambda) d\lambda \quad (4.1.2.5)$$

Φ_p – is a photon flux now, for the sake of new calculations to distinguish the difference of photon counts and J_{sc} is a short-circuit current. From that of above we now can see that:

$$J_{sc} = \int_{\lambda} \Phi_p(\lambda) \cdot R_\lambda \cdot \frac{hc}{\lambda} d\lambda \rightarrow \quad (4.1.2.6)$$

$$J_{sc}^{\text{rel}} = \int_{\lambda} \Phi_p^{\text{norm}}(\lambda) \cdot R_\lambda \cdot \frac{hc}{\lambda} d\lambda \quad (4.1.2.7)$$

where we have used relative value for short-circuit thanks to using a normalised values because of the fact that detector isn't ideal and that we can calculate the number of incident photons by simply using:

$$N_p = \frac{J_{sc}}{J_{sc}^{\text{rel}}} \quad (4.1.2.8)$$

From now we can clearly say that:

$$P_d = \int_{\lambda} \Phi_p^{\text{norm}}(\lambda) \cdot N_p \cdot \frac{hc}{\lambda} d\lambda \quad (4.1.2.9)$$

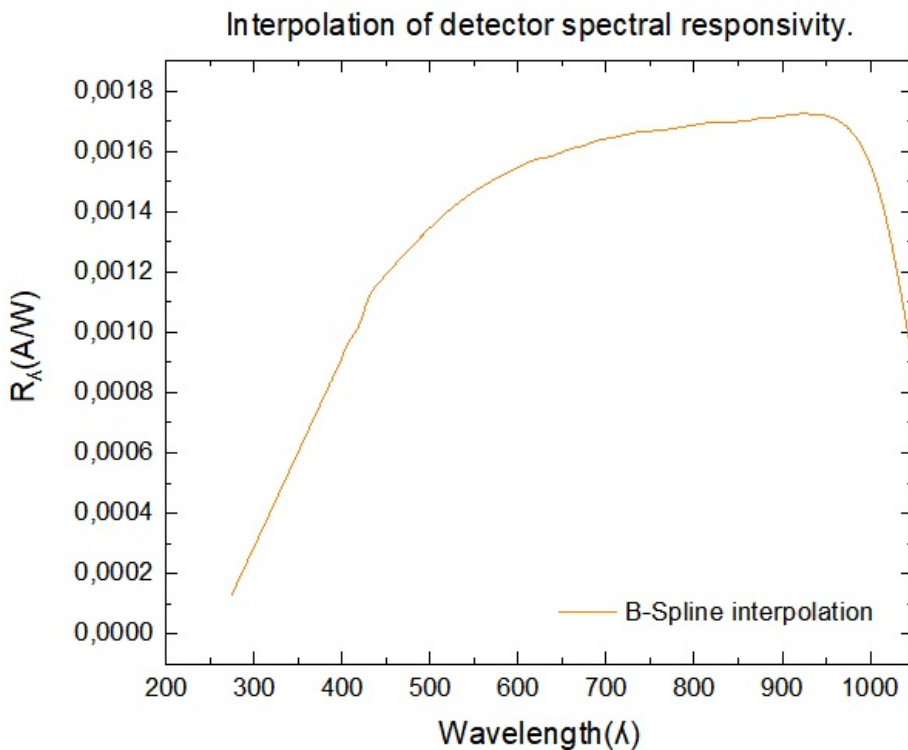


Figure 4.6: Original data from Gigahertz Optik GmbH

From integration and minding that $J_{sc} = 3,5 \cdot 10^{-4}$ mA we achieved that:

$$N_p \approx 1,4 \cdot 10^{21}$$

$$P_d \approx 2,71 \cdot 10^{-4} (W)$$

The calculations are roughly approximated and are just a presentation of methods used, mainly due to the fact that the full spectral characteristics weren't absolutely known. We can now estimate $P_{\text{density}} \approx \frac{P}{\Omega}$, where Ω is a solid angle. Therefore in our case from the information from Tab.(4.1) we can calculate PCEs of both photovoltaic devices by using:

	Detector	QDSC	Commercial Cell
Length from light source[mm]	400	75	603
Surface[mm ²]	36,32	27	462,8
Solid angle[sr]	2,27E-04	4,80E-03	1,27E-03
Incident Power [W]	2,72E-01	2,02E-03	3,47E-03

Table 4.1: Parameters of tested solar cells

$$PCE = \frac{V_m J_m}{P_{\text{in}}} \quad (4.1.2.10)$$

	V _m [V]	I _m [A]	P _{in} [W]	PCE
QDSC	0,32	6E-05	5,75E-03	0,33%
Commercial Cell	1,45	7E-05	1,53E-03	6,65%

Table 4.2: PCEs of photovoltaic devices

Provided producer of the Commercial Cell provides similar PCE compared to the given in 4.2 [8] we have estimated the values right. This means that our, certainly course, calculations show reasonable results from which we can definitely draw some conclusions.

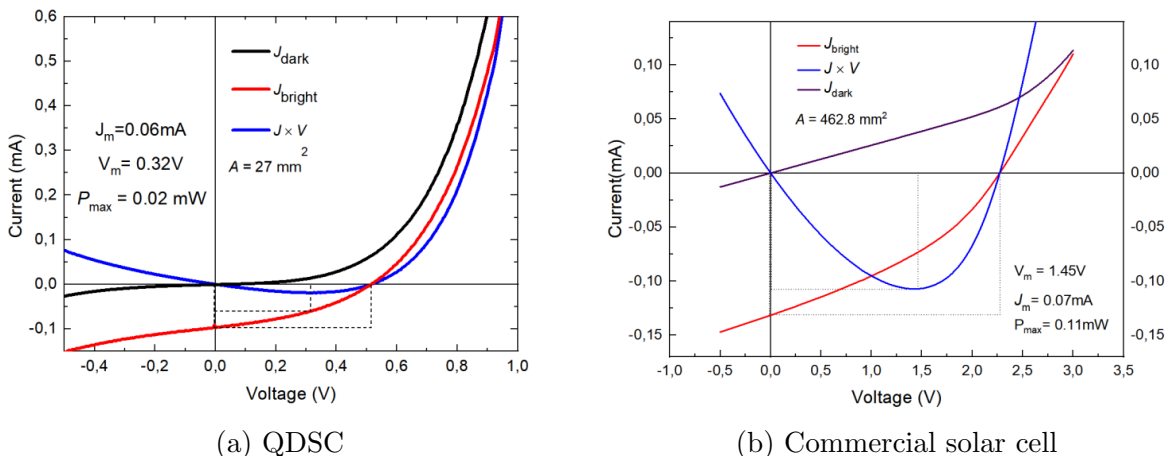


Figure 4.7: IV characteristics for QDSC and commercial cell

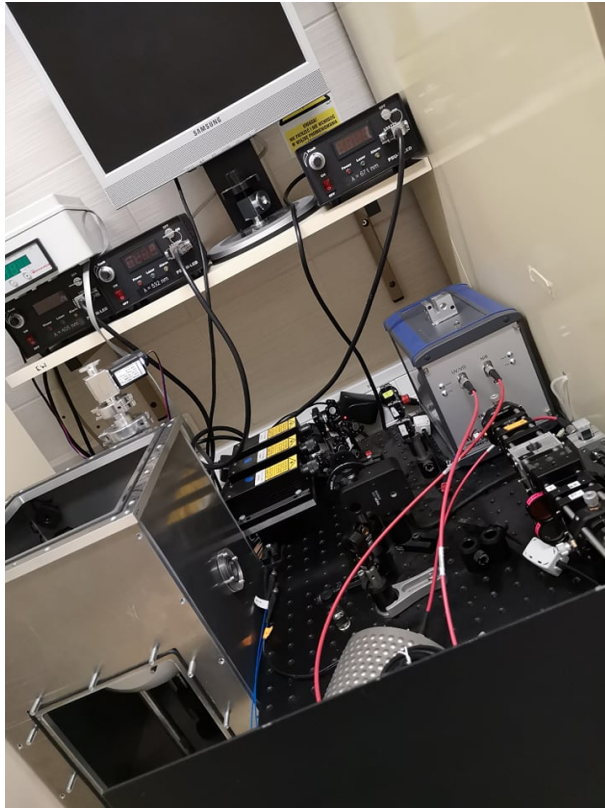


Figure 4.8: Laboratory absorption and photoluminescence measuring system

IMPROVEMENTS FOR THE FUTURE PROSPECTS

As we can clearly see, the PCE of QDSC made is small compared to the current world efficiencies [45]. This can be caused by numerous reasons. Working with colloidal quantum dots is always connected with the careful arrangements of various parameters. The slightest change of just one may provide a drastic change in the final result. Therefore we may conclude that the reason of such an efficiency is mostly challenged by the optimal choice of the layer width, quick degradation of QDs in the presence of air or physical defects on the device structure. The large leakage current may suggest that there are many defects inside the device structure which simply create traps for moving electrons. Nevertheless, the prospect of creating competitive QDSC is definitely in our reach. For example, we can see that I_{sc} is really more than satisfactory for device with such a small surface. Now, we have to deal with the improvement of our device. Optimization of the layer width and enlarging of CQDs stability will be the first things to do, but certainly not last. After testing those aspects, we may check if there is another way to exchange ligands in CQDs, which may provide major improvement in mobility, if there is growth of efficiency when changing or adding another transport layer in the device structure or if layer homogeneity can be further increased to stay comprehensive and competitive.

4.1.3 SECOND DEVICE MANUFACTURE

The first idea was to use different layers than previously. There were great quality PbSe QDs available. From that, we have made a similar device based on those QDs. Unfortunately, the outcome of the try was unfortunate and the device wasn't able to produce any current at all. Probably it was due to mismatch between the layers and poor layer deposition.

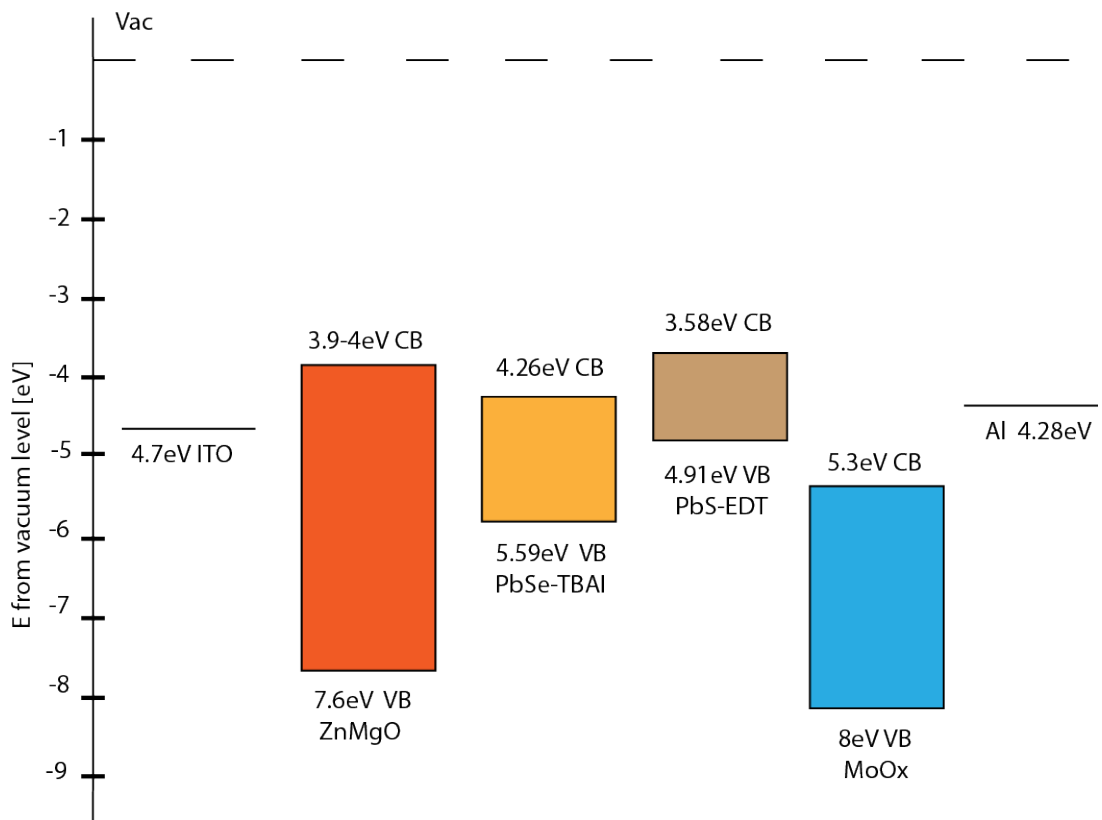


Figure 4.9: Energy structure of the first PbS-based QDSC

After that the second attempt of the same structure with PbS QDs was made, this time with bigger attention to fine deposition and shortened exposure to the air. Schematic of the device is very similar to it's former, except that the ZnO has been doped with Mg creating a layer of ZnMgO. However, we have used much different layer deposition times, which of course resulted in various layers width. This time also, the number of depositions was increased, also for EDT one. The purification method, which was used, has been described in Subsection(3.1.2) - using CHX/Acetonitrile. Later, we have achieved QDs with spectrum shown in Fig.(4.12). All the spectra have been created using the system shown in Fig.(4.8).

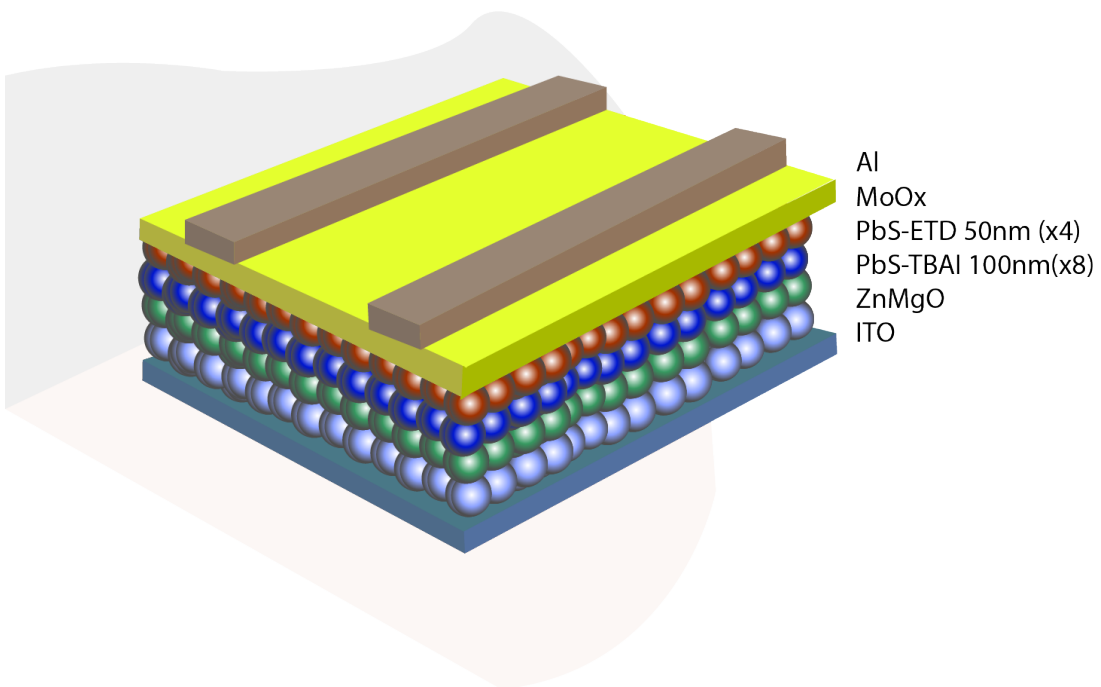


Figure 4.11: 3D structure of the first device based on PbS QDs

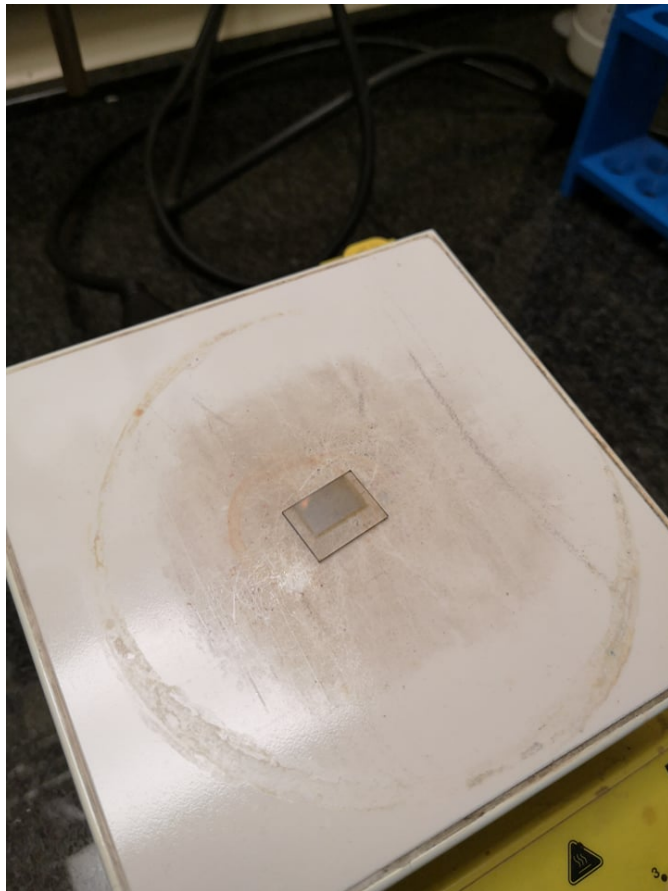


Figure 4.10: Cell heating

The layers were deployed using the spin-coater using this recipe from Fig. (4.13). After that, the last layer of MoOx has been deposited in the glove-box and the cell was heated

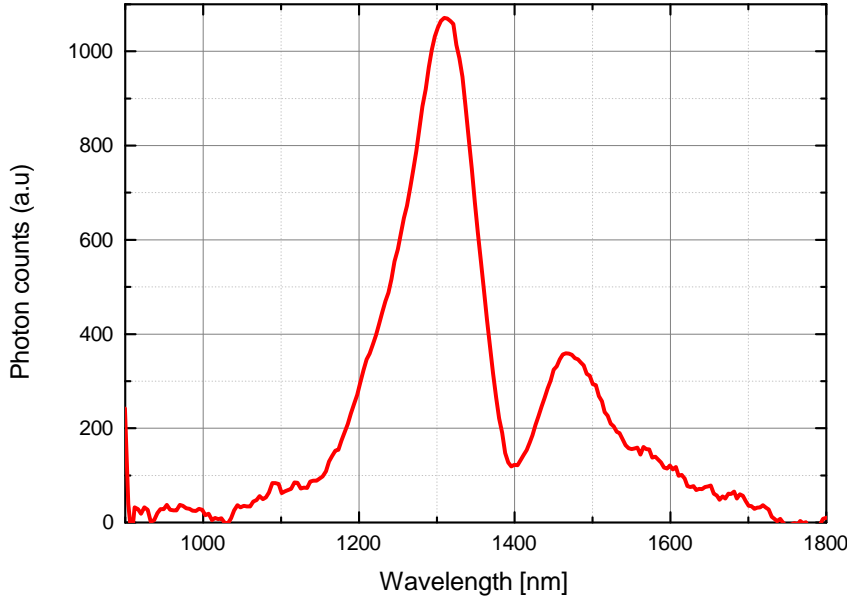


Figure 4.12: Photoluminescence of purified QDs

to get rid of solvents and, with it, some unwanted molecules. Then, with the last electrode has been deposited using the method described in the former chapter. Again the standard photovoltaic measurements were made.

On Fig.(4.12) we can see the photoluminescence of the purified QDs. Although it isn't perfect in the subject of the peak width, the greater peak is placed at suitable wavelength. It of course needs to be noted that the second peak is present because of the solvent absorption.

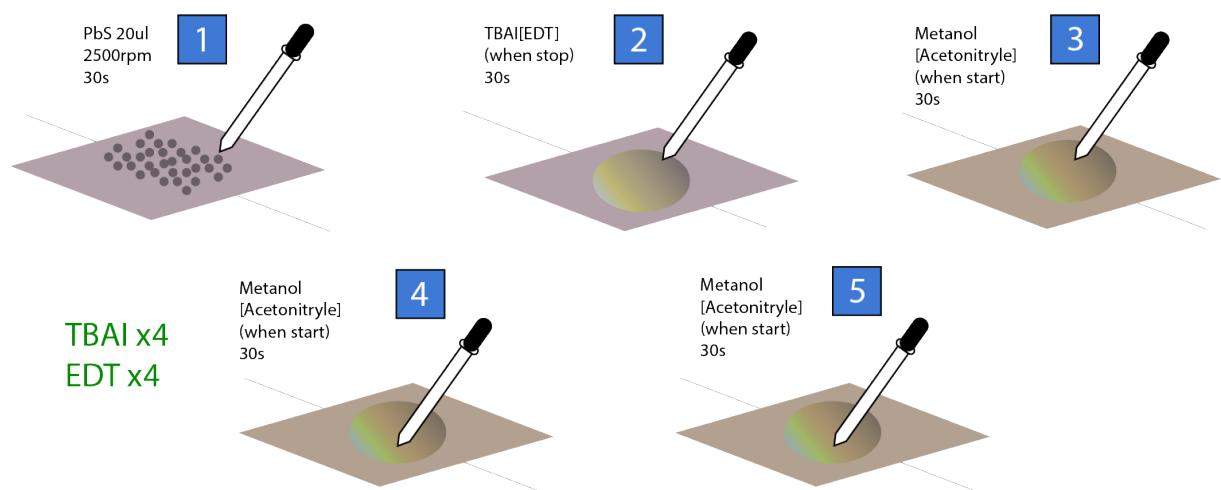
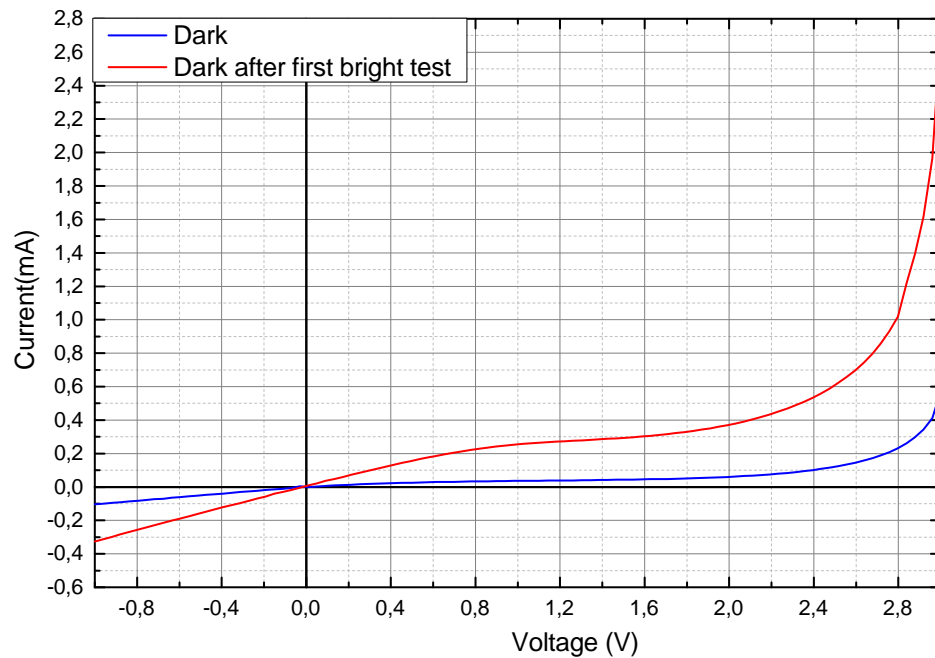
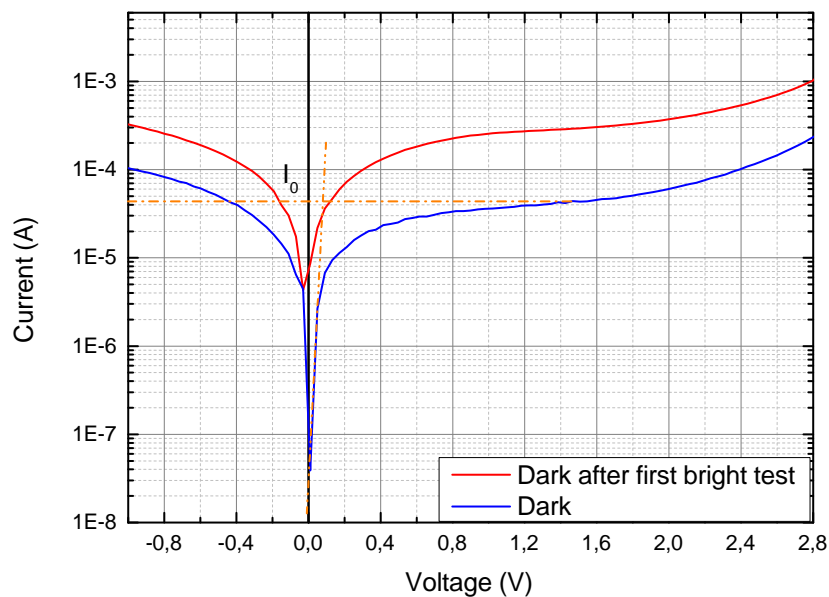


Figure 4.13: Second deposition parameters and number of depositions made



(a) Dark spectrum measured for the second time and after one test with bright spectrum



(b) Dark spectrum in logarithmic scale

Figure 4.14: Dark IV graph for the second device

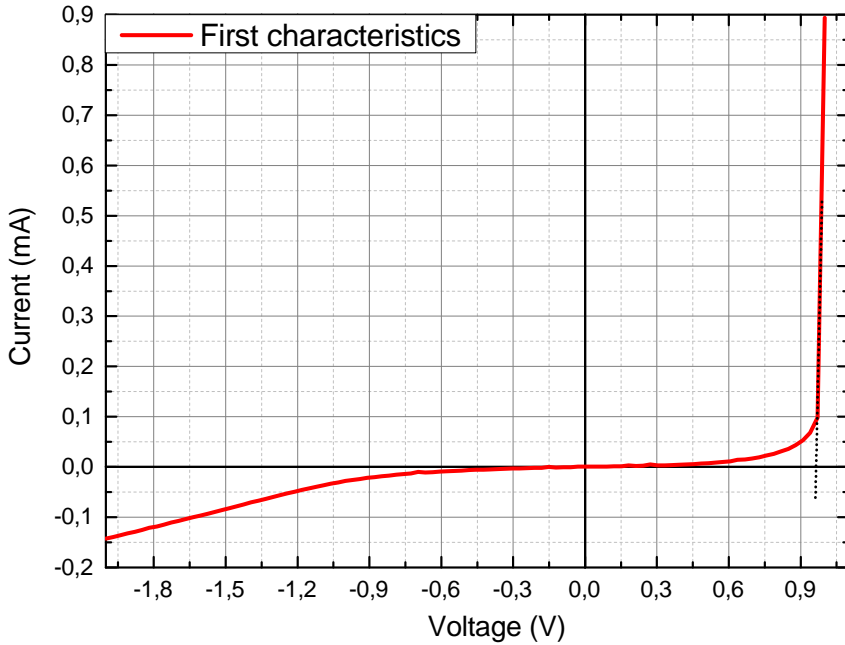


Figure 4.15: First results from dark IV characteristics

Firstly, the standard IV dark spectrum procedure has shown a quite promising characteristics Fig.(4.15). We can see, that there is a fine forward bias for the device, starting at $V_{bi} \approx 1V$. Nevertheless, the reverse bias shows an early beginning of a breakdown, which we have not expected. Probably, irreversible changes have been made to the device due to the reverse current and we will later see their effects. Additionally to that, the semi-logarithmic scale IV dark spectrum has been plotted in Fig.(4.14b). It is essential to calculate the series resistance.

After that, the verification of the destruction assumption has been tested. The conclusion is that the device hasn't been destructed completely, yet the beginning of the scope of forward current moved further in the voltage axis and the reverse current again behaved like Ohm-like characteristics. Later, we have checked the bright IV characteristics, with the power of three times the Sun(as the currents might be not sufficient enough for the precise measurement if the illumination was of just one Sun), and the rather surprising results are shown in Fig.(4.16) . To test how the lifetime of the device outlines, we have also shined at it for few minutes and tested the characteristics again. This, unfortunately, has destructed the device completely and I'm afraid this means that it's lifetime is rather scant. On the Fig.(4.16) we can see 3 tests for bright characteristics and one after the destruction. On Fig.(4.18) we can see the bright characteristics plotted for the current density.

From those figures we can see that the bright spectrum shows a rather flat but long trend. This means that the *Filling factor* will be small. The short-circuit current is $I_{sc} \approx 0,53mA$ and open-circuit voltage is $V_{oc} \approx 2,24V$. From that we can draw the power graph as well Fig.(4.17). It is crucial to provide the quantities to describe the device. Those are provided below in comparison table Tab.(4.3).

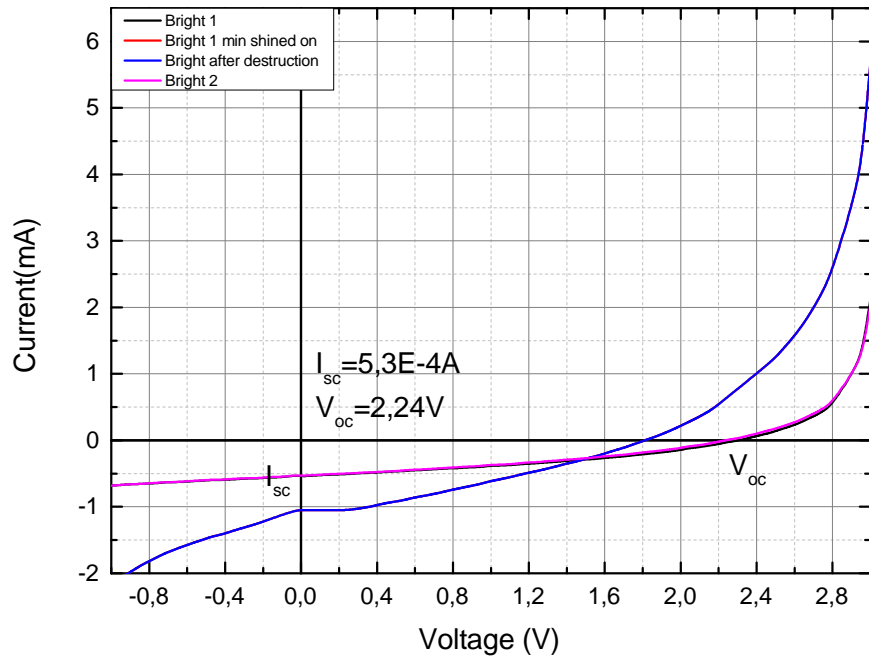


Figure 4.16: Bright IV characteristics. Note that the destructed device characteristics is not used and the values displayed are for the first test

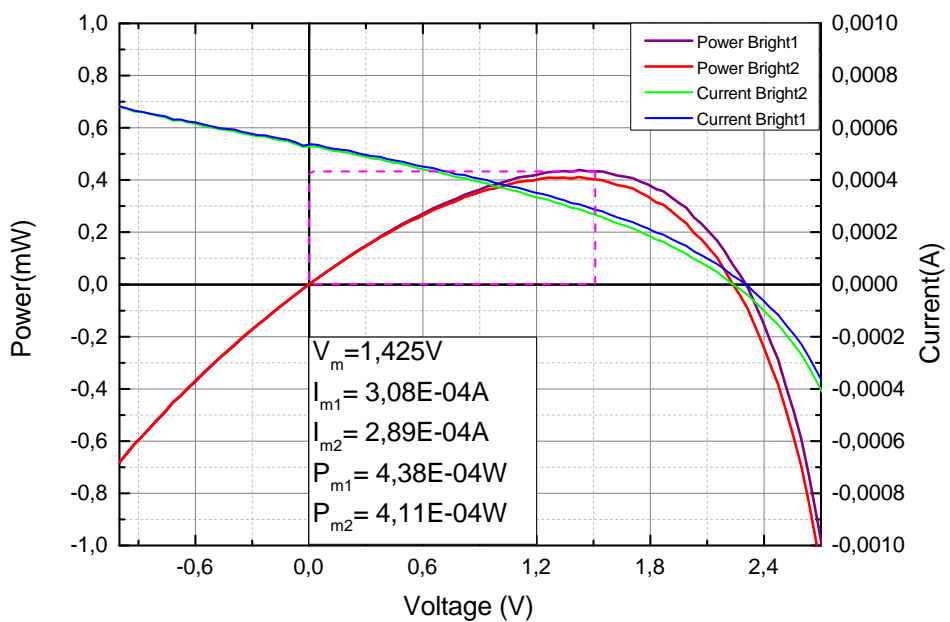


Figure 4.17: Power plotted for the first and second bright test. Maximal values of are plotted on the graph as well

	V _m [V]	I _m [A]	P _{in} [W]	PCE	V _{oc} [V]	I _{sc} [A]	FF
QDSC1	0,32	6E-05	5,75E-03	0,33%	0,51	1E-04	37,35%
Commercial Cell	1,45	7E-05	1,53E-03	6,65%	2,27	1,32E-04	33,90%
QDSC2	1,42	3,08E-04	5,75E-03	7,62%	2,24	5,32E-04	36,78%

Table 4.3: Comparison of all of the solar cells

The FF's of the devices were rather similar. Note that, we have stated that the I_{sc} of the former QDSC was really promising but the V_{oc} is small compared to the commercial device. This is not the case for the second PVD! With even bigger FF and similar V_m to the Commercial Solar Cell from the previous Table.(4.2), we have surpassed the device with rank greater I_m . This result is really uplifting. From the results above, we can also calculate the shunt and a series resistance if it is to allow us to calculate the generalized current. The shunt resistance can be calculated from the dark IV characteristic, because then you can be sure that no unwanted effects are present and we can achieve real response from material tested. We calculate the shunt resistance as inverse of the slope as $R_{sh} = \left(\frac{dI}{dU}\right)_{U=0}^{-1}$. Then we can also estimate the series resistance from the semi-logarithmic scale dark IV. It is derived from the deviation of the voltage at current after the exponential dependence isn't that important any more. We have achieved the values for $R_s \approx 2,11\Omega$ and $R_{sh} \approx 1,44 \cdot 10^4\Omega$. [94]

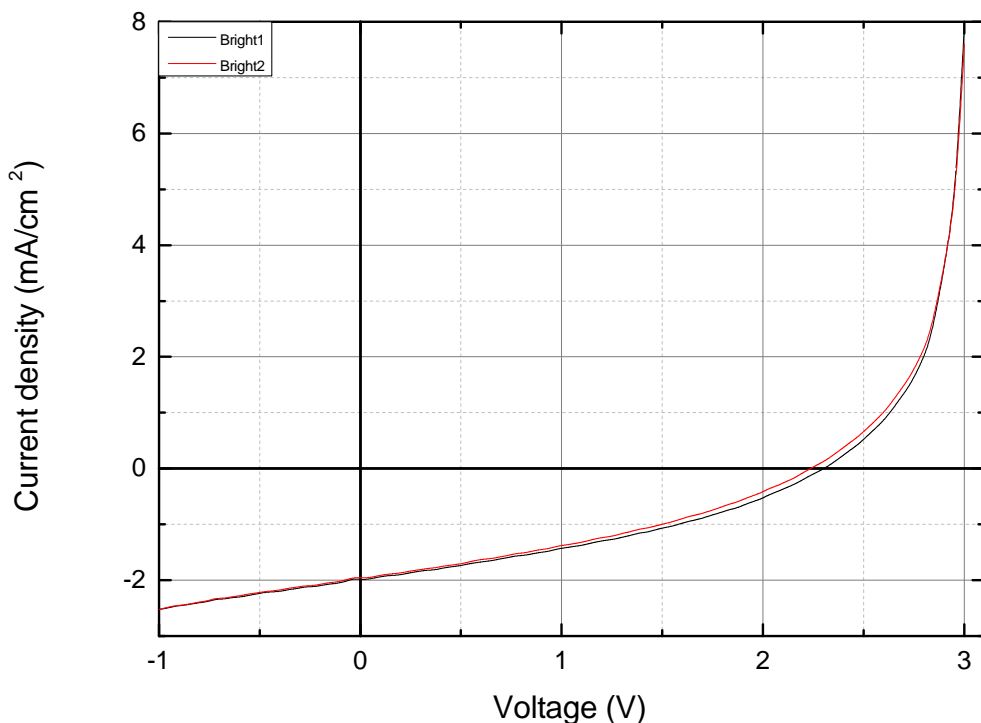


Figure 4.18: Useful figure for bright characteristics of current density

4.1.4 CONCLUSION AND OUTLOOK

We can now see that the big improvement of the device has been made when comparing to the first one. As it was based on the same method and structure, it is most probable that the layer width of the second device is more optimal. Another point is that the time spent on air exposure was probably too large for the first device and it might have suppressed its properties. Nevertheless, with some optimisation of the technique, the achievement of surpassing the commercial device is undeniable. As it is possibly not the last version of the device and the upgrades are ought to be provided in the future, there are plenty of possibilities to make it better. We have to say, that main problem of the device is a small FF and considerably short lifetime(in terms of device usage). One may think how to improve them. On the other hand, conclusion is that the biggest impact on the PCE of the device has been made by the placement of V_{oc} . We may also note that the stability in the air is due to imperfections of the manufacture, not the parameters of QD sensitizers because the potential stability of this alignment has been proven before[17]. Yet, this document also provides us with the information that air stability is essentially better without using the MoO_x layer. We may think about other hole extracting material with comparable optical and electric properties. There is also possibility of adding another layer between as it may provide some improvement and, as the valence band of MoOx depends on concentration of the oxygen we may test different layers of that. Some of the improvements in the PCE may be due to the better alignment of PbS-EDT and PbS-TBAI when compared to the previous one, as it has been proven to be crucial due to band offsets between them that block electrons coming to the anode, when simultaneously finely transporting holes. We can also potentially create better alignment between ZnMgO and PbS-TBAI with changing the Mg concentration(thus changing the optical bandgap). We could try to make other metallic contacts as well, to create better series resistance, as it will improve the FF. Better I_{sc} will surely be achieved with less defects inside the structure but there was no possibility to see any of the defect states, because of the absence of such measuring system. From the series resistance we can see that its effects are smaller than those of the shunt resistance. Therefore we conclude that to achieve a better FF and theoretically better PCE, we have to drastically reduce the shunt resistance(reduce current transport paths, defects etc.). After that, if the sufficiently narrow-luminescence width CQDs is achieved, we can think about multiple exciton generation. Another thing is to think about providing better carrier mobilities and try to extract the carriers before recombining.

CHAPTER 5

FUTURE POSSIBILITIES

Providing that the following thesis is only an introduction to the big world of semiconductor photovoltaic devices, there is a huge field of work still to be done. One can say that the information from the chapters included is only a grain of sand in the big dessert, therefore, in this final chapter, some possible areas that can improve the former thoughts will be stated. Promise, it won't be long, as the ideas come and go very fast in the physical world. From the general point of view, there is a lot of things that can be improved in the process of production only. The spin-coating method of creating layers has its pros and cons. We may think of possible changes in the way of making them. It is rather a functionalisation method which needs to be done after one can make a device which gives some results. Inside this process, there is also some way to manipulate the width of the layers, number of depositions, some new layers maybe. Then, after that, there is probably the urging need to apply new materials. I won't state any publications about that, as it has been stated before, but one might think of creating a hybrid devices, with many different layers of distinct materials as it can deal with some physical problems like recombination processes. Great possibilities approach thereby by designing nanostructure layers capable of multi exciton generation, as it is probably the biggest reason to study those material. To thoughtfully make the application of new materials possible and, of course, rather profitable, in my opinion, the necessity of theoretical work is irrefutable. As for this scale, the nonlinear light processes occur to be very important there is a need to discuss the effects and how to exploit them to our needs. Probably, the improving step would be to analyse firstly the theoretical concepts of transport properties, recombination possibilities and etc., for then to come up with numerical simulations of such materials, as most of the programs available today focus on standard type I solar cells. One can apply the non-equilibrium Green Functions theory for the transport properties (f.e. [10]). For me, it would be really interesting thing to consider, as that opens people's minds for the quicker thinking of new materials. Because of the scale, there is also a great connection of to nano-designing of the structures, to implement 2D confined structures and for sure to use metallic nano-particles, as plasmonics has began to mark its print on today's physics world(for sure it is useful as many things can be calculated analytically). Nevertheless, I hope that this entry work has pushed up some ideas with its general form and it will be later developed more...

BIBLIOGRAPHY

- [1] In: *J. Am. Chem. Soc.* 133 (5602 2011).
- [2] URL: https://www.researchgate.net/post/How_does_dimensionality_for_density_of_states_works.
- [3] URL: <http://hyperphysics.phy-astr.gsu.edu/hbase/Solids/dsem.html>.
- [4] URL: pveducation.org.
- [5] URL: [https://www2.pvlighthouse.com.au/resources/courses/altermatt/The%20Solar%20Spectrum/The%20global%20standard%20spectrum%20\(AM1-5g\).aspx](https://www2.pvlighthouse.com.au/resources/courses/altermatt/The%20Solar%20Spectrum/The%20global%20standard%20spectrum%20(AM1-5g).aspx).
- [6] URL: https://www.wikiwand.com/en/Quantum_dot.
- [7] URL: https://commons.wikimedia.org/wiki/File:Core-shell_types.png.
- [8] URL: <http://www.vimun.cn/en/index.asp>.
- [9] Ahmed L. Ning Abdelhady, Susanna M. Bakr Zhijun Thon, and Edward H. Sargent Graham H. Osman M. Carey. “Colloidal quantum dot solar cells”. In: *Chemical Reviews* (2015).
- [10] Urs Aeberhard. *Quantum-kinetic perspective on photovoltaic device operation in nanostructure-based solar cells*. IEK-5 Photovoltaik, Forschungszentrum Jülich, 52425 Jülich, Germany. 2017.
- [11] Daniel M. Balazs et al. “Comparing halide ligands in pbs colloidal quantum dots for field effect transistors and solar cells”. In: *ACS Applied nano materials* (2018).
- [12] Daniel M. Balazs et al. “Counterion-Mediated Ligand Exchange for PbS Colloidal Quantum Dot Superlattices”. In: *ACS Nano* 9.12 (Nov. 2015), pp. 11951–11959. DOI: 10.1021/acsnano.5b04547.
- [13] Emil Wolf Max Born. *Principles of optics - electromagnetic theory of propagation, interference and diffraction of light*. 1999.
- [14] G. Xiao C. Shi J. Chen and Z. Zhang L. Li. In: *Appl. Surf. Sci.* 410 (2017).
- [15] S. Hayase C.H.Ng H.N.Lim. “Photovoltaic performances of mono- and mixed-halide structures for perovskite solar cell: a review”. In: *Renewable and Sustainable Energy Reviews* (2018).
- [16] K. Cheng et al. In: *Chem. Commun* (2012).
- [17] Chia-Hao M. Chuang et al. “Improved performance and stability in quantum dot solar cells through band alignment engineering”. In: *Nature Materials* 13.8 (May 2014), pp. 796–801. DOI: 10.1038/nmat3984.
- [18] Gavin Conibeer. “Third-generation photovoltaics”. In: *Materialstoday* (2007).

- [19] Niklas Cordes et al. “Passivation of pbs quantum dot surface with l-glutathione in solid-state quantum-dot-sensitized solar cells”. In: *Applied Materials & Interfaces* (2016).
- [20] Z. Du et al. In: *J. Am. Chem. Soc.* 138 (2016).
- [21] C. Ribeiro E. R. Leite. *Crystallization and growth of colloidal nanocrystals*. Springer, 2012.
- [22] L. Esaki and R. Tsu. “Superlattice and Negative Differential Conductivity in Semiconductors”. In: *IBM Journal of Research and Development* 14.1 (Jan. 1970), pp. 61–65. doi: 10.1147/rd.141.0061.
- [23] Ikerne Etxebara, Jon Ajuria, and Roberto Pacios. “Polymer fullerene solar cells materials processing issues and cell layouts to reach power conversion efficiency over 10 percent”. In: *Jorunal of Photonics for Energy* (2015).
- [24] James Z. Fan et al. “Mixed-quantum-dot solar cells”. In: *Nature Communications* ().
- [25] Mark Fox. *Optical properties of Solids*. Springer.
- [26] M. A. Hines G.D. Scholes. “Colloidal PbS nanocrystals with size-tunable near-infrared emission: observation of post-synthesis self-narrowing of the particle size distribution.” In: *Adv. Mater* 15 (2003).
- [27] Wenhui Gao et al. “Towards understanding the initial performance improvement of PbS quantum dot solar cells upon short-term air exposure”. In: *RSC Advances* 8.27 (2018), pp. 15149–15157. doi: 10.1039/c8ra01422a.
- [28] K. Qiao Gong Jiawei Sumathy, Qiquan Zhou, and Zhengping. “Review on dye-sensitized solar cells (dsscs): advanced techniques and research trends”. In: *Renewable and Sustainable Energy Reviews* (2017).
- [29] Victoria Gonzalez-Pedro et al. “Enhanced Carrier Transport Distance in Colloidal PbS Quantum Dot-Based Solar Cells Using ZnO Nanowires”. In: *The Journal of Physical Chemistry* (2015).
- [30] Ryan M. France Matthew O. Reese Sanjini U. Nanayakkara Bradley A. MacLeod Dmitri V. Talapin Matthew C. Beard Gregory F. Pach J. Matthew Kurley and Joseph M. Luther Ryan W. Crisp. “Tandem solar cells from solution-processed CdTe and PbS quantum dots using a ZnTe/ZnO tunnel junction”. In: *Nano Letters* (2017).
- [31] P. Guyot Sionnest. “Electrical transport in colloidal quantum dot films.” In: *J. Phys. Chem. Lett.* 3 (2012), pp. 1169–1175.
- [32] *How Much Solar Energy Can We Harvest?* URL: <http://home.iprimus.com.au/nielsens/solen.html>.
- [33] <https://ourworldindata.org/energy-production-and-changing-energy-sources>. 2019.
- [34] Andreas Mandelism Xinzhen Lan Lilei Hu. “Imbalanced charge carrier mobility and schottky junction induced anomalous current-voltage characteristics of excitonic pbs colloidal quantum dot solar cells”. In: *Solar Energy Materials and solar cells* (2016).
- [35] Juan Bisquert Huashang Rao Ivan Mora-Sero and Xinhua Zhong Zhenxiao Pan. “Quantum dot-sensitized solar cells”. In: *Chem. Soc. Rev* 47/7659 (2018).

- [36] J. Bisquert I. Mora-Sero F. De Angelis and P. Wang Y. Bai. In: *Chem. Rev* 114 (2014).
- [37] S. Ikeda et al. In: *Renewable Sustainable Energy Rev* (2014).
- [38] Ivan Infante et al. “darker-than-black’ pbs quantum dots: enhancing optical absorption of colloidal semiconductor nanocrystals via short conjugated ligands”. In: *Journal of the American Chemical Society* (2015).
- [39] Energy Insights. *Global Energy Perspective 2019: Reference Case*. Tech. rep. Insights, Energy, 2019.
- [40] D. Long W. Jiang Z. Pan Y. Li J. Du Z. Du and X. Zhong S. Jiao. In: *J. Phys. Chem. Lett* 8 (2017).
- [41] K. Yan J. Qiu and S. Yang Z. Zhu. In: *ACS Appl. Mater. Interfaces* (2013).
- [42] John David Jackson. *Classical Electrodynamics*.
- [43] Yi Li Zhipeng Shao Yafeng Xu Jun Zhu Yang Huang and Songyuan Dai Mei Lv. “Colloidal CuInS₂ Quantum Dots as Inorganic Hole-transporting”. In: *ACS Applied Materials & Interfaces* (2015).
- [44] D. R. Baker Kamat. In: *Adv. Funct. Mater* 19 (2009).
- [45] Prashant V. Kamat. “Quantum dot solar cells. the next big thing in photovoltaics”. In: *The Journal of Physical Chemistry Letters* (2018).
- [46] Victor I. Klimov. *Nanocrystal quantum dots*. CRC Press.
- [47] Haibin Wang andTakaya Kubo et al. “Efficiency Enhancement of PbS Quantum Dot/ZnO Nanowire Bulk-Heterojunction Solar Cells by Plasmonic Silver Nanocubes”. In: *ACS Nano* (2015).
- [48] C. Fei X. Liu Z. Zhao Y. Wang L. Lv X. Wang and G. Cao J. Tian. In: *J. Phys. Chem. C*, (2014).
- [49] C. Fei L. Lv, X. Liu Y. Wang, and J. Tian Cao. In: *J. Mater. Chem. A* (2014).
- [50] Y. L. Lee and Y. S. Lo. In: *Adv. Funct. Mater.*, (2009).
- [51] Hosub Lim et al. “Continuous purification of colloidal quantum dots in large-scale using porous electrodes in flow channel”. In: *Scientific reports* () .
- [52] S. M. Ali M. A. Manthrammel W. A. Farooq and M. Atif A. Fatehmulla. In: *J. Nanomater.* (358063 2015).
- [53] Rachel S. Hoffman Ferry Prins Mark C. Weidman Megan E. Beck and William A. Tisdale. “Monodisperse air-stable PbS nanocrystals via precursor stoichiometry control”. In: *ACS Nano* (2014).
- [54] Andrea Maurano et al. “Photovoltaic performance of pbs quantum dots treated with metal salts”. In: *ACS Nano* (2016).
- [55] Meteotest AG. (1991-2010).
- [56] Jin Wang Mikhail Artemyev and Jianguo Tang Zhonglin Du. “Performance Improvement Strategies for Quantum Dot Sensitized Solar Cells: A Review”. In: *Journal of Materials Chemistry A* (2019).

- [57] Hui Yang Qing Zhou Huibiao Liu Xinzhen Lan Mengxia Liu Jizheng Wang Edward H. Sargent Mingjian Yuan Hui Li and Yuliang Li Zhiwen Jin. “Graphdiyne: An Efficient Hole Transporter for Stable High-Performance Colloidal Quantum Dot Solar Cells”. In: *Materials Views* (2016).
- [58] N. D. Mermin N. W. Ashcroft. *Solid state physics*. Ed. by Cornell University. 1976.
- [59] Nasa. <https://climate.nasa.gov/evidence/>. 2019.
- [60] Guangda Niu, Xudong Guo, and Liduo Wang. “Review of recent progress in chemical stability of perovskite solar cells”. In: *Journal of Materials Chemistry A* (2014).
- [61] Mengxia Liu Jixian Xu Andrew H. Proppe Grant Walters Fengjia Fan Hairen Tan Min Liu Zhenyu Yang Sjoerd Hoogland Oleksandr Voznyy F. Pelayo García de Arquer and Edward H. Sargent Xinzhen Lan. “10.6 percent certified colloidal quantum dot solar cells via solvent- polarity-engineered halide passivation”. In: *ACS Nano Letters* (2016).
- [62] Pongsakorn Kanjanaboops Oleksandr Voznyy David Zhitomirsky and Edward H. Sargent Mingjian Yuan. “ynergistic Doping of Fullerene Electron Transport Layer and Colloidal Quantum Dot Solids Enhances Solar Cell Performance”. In: *Adv. Mat.* (2014).
- [63] L. Qu P. Zhao X. Zhao and X. Lai S. Yang. In: *J. Mater. Chem A*. (2015).
- [64] Alex Valavanis Paul Harrison. *Quantum Wells, Wires and Dots Theoretical and Computational Physics of Semiconductor Nanostructures*. Wiley.
- [65] Ewa Placzek-Popko. “Wykład II Fotoluminescencja”. Politechnika Wrocławska.
- [66] planck. “Distribution of energy in the spectrum”. In: *Annalen der Physik* 4 (1901), pp. 553–563.
- [67] Nikola Prodanovic. “Semiconductor Quantum Dots: Intraband Electronic, Optical and Carrier Dynamical Properties”. PhD thesis. The University of Leeds School of Electronic and Electrical Engineering, Jan. 2014.
- [68] M. D. Regulacio and M.-Y. Han. “Composition-Tunable Alloyed Semiconductor Nanocrystals”. In: *Acc. Chem. Res.* 43 (2010).
- [69] *Renewables Information*. 2018.
- [70] Weijian Chen Zhilong Zhang Lin Yuan Zihan Chen Gavin J. Conibeer Gang Wang Robert J. Patterson Yicong Hu and Shujuan Huang Long Hu. “High Performance PbS Colloidal Quantum Dot Solar Cells by Employing Solution-Processed CdS Thin Films from a Single-Source Precursor as the Electron Transport Layer”. In: *Adv. fun. mat.* (2017).
- [71] R. Gomez Q. Shen T. Toyoda S. Gimenez F. Fabregat-Santiago and I. Mora-Sero J. Bisquert. In: *Acc. Chem. Res.* 42 (2009).
- [72] Yuequn Shang et al. “Colloidal Quantum Dot Ligand Engineering for High Performance Solar Cells”. In: *Royal Society of Chemistry* (2016).
- [73] Yi Shen, Megan Y. Gee, and A. B. Greytak. “Purification technologies for colloidal nanocrystals”. In: *Chemical Communications* 53.5 (2017), pp. 827–841. DOI: 10.1039/c6cc07998a.
- [74] W. Shockley and Queisser. “Detailed Balance Limit of Efficiency of p-n Junction Solar Cells”. In: *Journal of Applied Physics* 32 (1961), pp. 510–519.

- [75] Robert Pattersonb Shujuan Huangb and Jonathan E. Halperta Long Hua. “Enhanced mobility in PbS quantum dot films via PbSe quantum dot mixing for opto-electronic applications”. In: *Journal of Materials Chemistry C* (2019).
- [76] Jung Hoon Song and Sohee Jeong. “Colloidal quantum dot based solar cells: from materials to devices”. In: *Nano Convergence* (2017).
- [77] Rafał Świętek. Bachelor’s thesis. 2020.
- [78] S. M. Sze. *Physics of the semiconductor devices*. Wiley.
- [79] J. Tian and G. Cao. In: *J. Phys. Chem. Lett* 6 (2015).
- [80] K. Tvrdy et al. In: *J. Am. Chem. Soc* 130 (2008).
- [81] W. Xue L. Zhang L. Zhao Y. Li W. Feng J. Du and X. Zhong W. Wang. In: *Adv. Mater* (2018).
- [82] Liang Wang et al. “6.5 percent certified sb₂se₃ solar cells using pbs colloidal quantum dot film as hole transporting layer”. In: *ACS Energy Letters* (2017).
- [83] Ulrike Woggon. *Optical Properties of Semiconductor Quantum Dots*. Springer.
- [84] Jiang Wu and Zhiming M. Wang, eds. *Quantum Dot Solar Cells*. Springer New York, 2014. DOI: 10.1007/978-1-4614-8148-5.
- [85] Q. Liu C. He X. Liu X. Gao X. Hong and M. Ye C. Lin. In: *Sustainable Energy Fuels* (2017).
- [86] Suping Jia Jianhui Dong Jianfeng Zheng Jianghong Zhao Zhijian Wang Li Li Li Zhang Xin Meng Huijuan Cui and Zhenping Zhu Yanyan Zhu. “Graphene Frameworks Promoted Electron Transport in Quantum Dot-Sensitized Solar Cells”. In: *Appl. Mater. Interfaces* (2014).
- [87] K. Chen Y. Cheng Y. Liu Y. Zhao and W. Chen Z. Peng. In: *Electrochim. Acta* 135 (2014).
- [88] X. F. Gao Q. Chen Y. Yu H. Y. Pan and L. M. Peng W. T. Sun. In: *J. Am. Chem. Soc* (2008).
- [89] A. Yamada, S. Tamura Shen, and T. Toyoda. In: *Appl. Phys. Lett.* 97 (2010).
- [90] Xichuan Yang et al. “Stable and efficient pbs colloidal quantum dot solar cells incorporating low-temperature processed carbon paste counter electrodes”. In: *Solar Energy* (2017).
- [91] Guozheng Shi Zeke Liu Kunyuan Lu Lu Han Xufeng Ling Han Zhang Si Cheng Yong jie Wang Qipeng Liu and Wanli Ma Si Chen. “Broadband Enhancement of PbS Quantum Dot Solar Cells by the Synergistic Effect of Plasmonic Gold Nanobipyramids and Nanospheres”. In: *Advanced Science News* (2017).
- [92] W. W. Yu et al. “Experimental Determination of the Extinction Coefficient of CdTe, CdSe, and CdS Nanocrystals.” In: *Chem. Mater* (2003).
- [93] Donghuan Qin Yangdong Zhang Yuehua Yang Miaozi Li and Lintao Hou Rongfang Wu. “Solvent Engineering for High-Performance PbS Quantum Dots Solar Cells”. In: *Nanomaterials* (2017).
- [94] A. Zekry and A.Y. Al-Mazroo. “A distributed SPICE-model of a solar cell”. In: *IEEE Transactions on Electron Devices* 43.5 (May 1996), pp. 691–700. DOI: 10.1109/16.491244.

- [95] Huihui Zhang et al. “Recent advances of critical materials in quantum dot–sensitized solar cells. a review”. In: *Royal Society of Chemistry* (2015).
- [96] Nanlin Zhang et al. “P3HT as a Hole Transport Layer for Colloidal”. In: *ACS Applied Materials & Interfaces* (2016).
- [97] Q. Zhang et al. In: *Energy Environ. Sci.*, (2013).